https://doi.org/10.5194/egusphere-2026-914
Preprint. Discussion started: 11 March 2026

Aerosol processing during long-range transport governs the chemical composition of haze over the northern Indian Ocean

Karin Stegelius[1], Pauline Thompson[1], Pia Karbiener[1,*], Piotr Markuszewski[1,2,3], Andre S. H. Prevot[4], Sachchida N. Tripathi[5,6], Claudia Mohr[4,7], Liine Heikkinen[1,2], Krishnakant Budhavant[8,9] and Sophie L. Haslett[1,2]

[1]Department of Environmental Science, Stockholm University, Stockholm, Sweden
[2]Bolin Centre for Climate Research, Stockholm University, Stockholm, Sweden
[3]Physical Oceanography Department, Institute of Oceanology, Polish Academy of Sciences, Sopot, Poland
[4]PSI Center for Energy and Environmental Sciences, Paul Scherrer Institute, Villigen PSI, Switzerland
[5]Department of Civil Engineering, Indian Institute of Technology Kanpur, Kanpur, India
[6]Department of Sustainable Energy Engineering, Indian Institute of Technology Kanpur, Kanpur, India
[7]Department of Environmental Systems Science, ETH Zurich, Zürich, Switzerland
[8]Maldives Climate Observatory at Hanimaadhoo, Hanimaadhoo, Maldives
[9]Divecha Centre for Climate Change, Indian Institute of Science, Bangalore, India

[*]*now at* Department of Environmental Sciences, University of Basel, Basel, Switzerland

Correspondence to: Sophie L. Haslett (sophie.haslett@aces.su.se) and Krishnakant Budhavant (kbbudhavant@gmail.com)

Abstract. Each year during the winter period, a persistent haze forms over the Indian subcontinent and the northern Indian Ocean. This has been shown to influence regional warming, rainfall patterns and air quality. Previous studies have demonstrated that this haze is largely anthropogenic in origin, with its composition dominated by sulfate, organic compounds and black carbon. Nevertheless, to date, information about its composition has largely been limited to bulk chemical composition and low time-resolution data. Here, we aim to characterise aerosol composition over the Indian Ocean on the molecular level, in order to identify the impact of different sources and processing in this region. High-time-resolution measurements were conducted at the Maldives Climate Observatory, Hanimaadhoo (MCOH) using a Time-of-Flight Aerosol Mass Spectrometer (AMS) and Chemical Ionisation Mass Spectrometer with a Filter Inlet for Gases and Aerosols (FIGAERO-CIMS). Results showed a remarkably uniform composition, despite variability in source regions and total concentration, indicating strong regional mixing of air masses. Sulfate accounted for approximately 52% of non-refractory sub-micron particulate mass. Eighteen sulfur-containing organic compounds were identified, some for the first time in this location. Tracers of some sources, particularly biomass burning, were identified in the organic mass spectrum. However, the majority of organic mass was dominated by highly-processed compounds such as dicarboxylic acids. Our results underscore the impact of long-range transport and heterogeneous sulfate-driven chemistry on aerosol composition over the Indian Ocean, with important implications for understanding radiative forcing, aerosol-cloud interactions, and regional climate feedbacks in South Asia.

https://doi.org/10.5194/egusphere-2026-914
Preprint. Discussion started: 11 March 2026

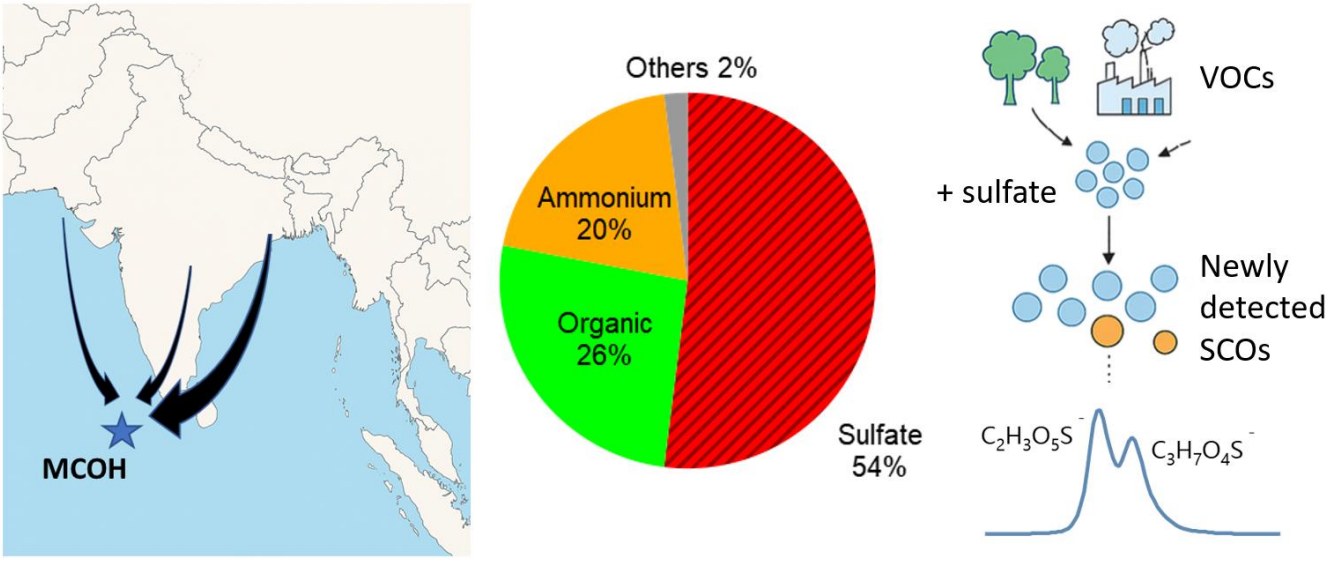

1 Introduction

The South Asian wintertime meteorological conditions and high levels of emissions create a large anthropogenic haze each year, which stretches across the northern Indian Ocean, India and Pakistan (Bharali et al., 2019; Budhavant et al., 2024; Dasari et al., 2025). This has large implications for air quality, the radiation budget and climate (Nair et al., 2023). It reduces air quality and visibility across this large region, in addition to dimming the surface and warming the atmosphere (Krishnan and Ramanathan, 2002). During the dry season (typically January–March), this aerosol is blown across the Indian Ocean to the Maldives from the South Asian subcontinent (Budhavant et al., 2018; Ramachandran and Rupakheti, 2020). The transported aerosol mass contains a large fraction of sulfate, but is also characterised by high concentrations of organic aerosol and absorbing aerosol such as black and brown carbon (Budhavant et al., 2018, 2024; Ramachandran and Rupakheti, 2020). This air contains more aerosol mass in the fine mode than in the coarse mode (Budhavant et al., 2023). Fine mode aerosols, in particular, contribute substantially to aerosol optical depth over the Indian Ocean (Budhavant et al., 2023; Ramachandran and Rupakheti, 2020).

Previous studies indicate that this aerosol is predominantly anthropogenic in origin (Aswini et al., 2020; Budhavant et al., 2018; Ramana and Ramanathan, 2006), as evidenced during the COVID-19 pandemic in 2020 (Nair et al., 2023). Lockdowns and restrictions were imposed to minimise crowds and travel worldwide. Following this, there was a rapid and substantial decrease in transport and emissions activity. In the Indo-Gangetic Plain (IGP), the restrictions led to an 18% decrease in aerosol loading relative to the two earlier years, thereby increasing the solar radiation reaching the Earth's surface by 7% (Nair et al., 2023).

https://doi.org/10.5194/egusphere-2026-914
Preprint. Discussion started: 11 March 2026

Sulfate and organic compounds dominate the fine-mode non-refractory aerosol fraction over the Indian Ocean during winter (Budhavant et al., 2024; Dasari et al., 2019). Sulfate aerosol, being highly scattering, imposes a direct climate cooling effect in the region. In addition, the ability of sulfate aerosol particles to act as efficient cloud condensation nuclei (CCN) results in increased cloud albedo, which causes an even greater climate cooling effect. The negative radiative forcing from sulfate aerosol has been estimated to be substantial since pre-industrial times (Szopa et al., 2023).

The relative contribution of different sulfate sources over the Indian Ocean is at present poorly constrained. It is important to clarify this, as the ratio of anthropogenic to biogenic sulfate determines the extent to which changes in emission patterns will alter aerosol properties, with implications for the magnitude of future aerosol radiative forcing in the region. Previous studies have indicated that the majority of sulfate found over the Indian Ocean during the dry season is anthropogenic in origin (Budhavant et al., 2024; Clarke et al., 2025). However, contributions from non-anthropogenic sources have so far received little attention, perhaps due to the currently overwhelming dominance of anthropogenic sulfate. Dimethyl sulfide (DMS) produced by phytoplankton oxidises to form methane sulfonic acid (MSA) and sulfate in the atmosphere (Charlson et al., 1987; von Glasow and Crutzen, 2004; Granat et al., 2010; Leck et al., 1990). In addition, sulfur-containing organic aerosol (SCO) has been found to account for 1% of particulate matter mass concentration smaller than 2.5 μm in diameter ($PM_{2.5}$) over the Maldives, located in the northern Indian Ocean (Stone et al., 2012). Although SCOs have been found to contribute to aerosol mass in this region, only one study has examined their chemical composition in detail (Stone et al., 2012). Attaining a greater understanding of SCOs and the importance of DMS-derived sulfur over the Indian Ocean is critical for reducing the uncertainties in aerosol forcing estimates when anthropogenic sulfur contribution declines over the region due to air pollution mitigation.

Organic aerosol (OA) over the Indian Ocean represents a complex mixture of primary and secondary carbonaceous compounds originating from both continental and marine sources (Novakov et al., 2000; Papazian et al., 2022). This aerosol has a considerable impact on atmospheric optical properties (Nair et al., 2023; Satheesh et al., 1999; Srinivas and Sarin, 2013). Extensive field campaigns, including INDOEX and SAPOEX, along with recent shipborne measurements and ongoing observations at the site, have demonstrated that OA concentrations over the Indian Ocean are among the highest recorded in remote marine regions. However, these measurements have been restricted to bulk OA, or to specific groups of species such as alkanes or PAHs (eg Sheesley et al., 2011). Organic aerosol is particularly challenging to characterise because it is composed of thousands of different compounds, which encompass a large range of chemical properties and volatilities. These undergo different processes in the atmosphere and can have different environmental and health impacts. The majority of aerosol observed over the Indian Ocean during the winter season originates from the Indian continent and, in particular, the highly-polluted Indo-Gangetic Plain, which contains several large cities, including the Indian capital, Delhi (Dasari et al., 2025; Ramana and Ramanathan, 2006). These aerosols will undergo processing during transport, but the impact of this processing on aerosol composition over the remote Indian Ocean remains poorly understood. A comprehensive chemical characterisation remains lacking in this region.

https://doi.org/10.5194/egusphere-2026-914
Preprint. Discussion started: 11 March 2026

In this study, we assess the contributions of various sources and chemical species to sulfate and organic aerosols at the MCOH site. Utilising simultaneous measurements from a High-Resolution Time-of-Flight Aerosol Mass Spectrometer (HR-ToF-AMS, hereafter AMS) and an Iodide High-Resolution Time-of-Flight Chemical Ionisation Mass Spectrometer coupled with a Filter Inlet for Gases and Aerosols (I-HR-ToF-FIGAERO-CIMS, hereafter CIMS), we present a detailed source apportionment and determine aerosol mass concentrations with high temporal resolution. The CIMS uses soft ionisation to identify specific chemical species, including SCOs and OA, thereby providing an in-depth understanding of the different compounds that make up both SCO and OA populations. Our primary objective is to identify the main compounds that contribute towards sulfate and organic aerosol at MCOH, and to use these results to explain more about the most important sources and influences on aerosol chemistry and composition in this region. To our knowledge, this work marks the first application of high-time-resolution, high-mass-resolution, soft-ionisation in situ mass spectrometry at this field site, providing fresh insights into the dynamic processes that govern sulfate and organic aerosol formation and transformation in the Indian Ocean region.

2 Methods

2.1 Description of the field campaign and sampling site

The field campaign took place during the dry winter monsoon season, which is characterised by northeasterly winds originating from the Indian subcontinent (Budhavant et al., 2018, 2024; Ramachandran and Rupakheti, 2020). This air mass is typically influenced by South Asian winter time air pollution and passes over the Indian Ocean before reaching the Maldives (Budhavant et al., 2018, 2024). The Maldives is located near the equator and maintains a relatively stable temperature throughout the year. The dry season typically experiences limited rainfall.

2.2 Back trajectory and fire count analysis

Air-mass backward trajectories (AMBTs) were calculated using the Hybrid Single-Particle Lagrangian Integrated Trajectory (HYSPLIT) model (version 4), developed by the National Oceanic and Atmospheric Administration (NOAA) (Draxler and Hess, 1998; Stein et al., 2015). The model used CDC1 meteorological data to investigate possible transport pathways to the receptor site, as illustrated in Figures 1c and S2. Ten-day backward trajectories were computed for the sampling location at 00:00, 06:00, 12:00, and 18:00 UTC, allowing for an assessment of both regional and long-range air-mass origins. Cluster analysis was used to group trajectories with comparable transport pathways and to identify the dominant airflow patterns influencing the sampling station. As shown in Figure 1c, most trajectories originate in South Asia before reaching the receptor site.

To evaluate the impact of biomass burning, satellite-derived fire-count data were integrated into the analysis (Figure 1c). Fire hotspots detected by the Moderate Resolution Imaging Spectroradiometer (MODIS) were spatially overlaid with the backward trajectories for each identified transport phase (Giglio et al., 2016). This integrated approach enhances the identification of major source regions and transport processes affecting the receptor site.

https://doi.org/10.5194/egusphere-2026-914
Preprint. Discussion started: 11 March 2026

2.3 Instrumentation

A High-Resolution Time-of-Flight Aerosol Mass Spectrometer (HR-ToF-AMS, hereafter AMS; Aerodyne Research Inc., Billerica, MA, USA; Canagaratna et al., 2007; DeCarlo et al., 2006; Onasch et al., 2012) and an Iodide-Reagent, High-Resolution Time-of-Flight Chemical Ionisation Mass Spectrometer equipped with a Filter Inlet for Gases and Aerosols (I-ToF-FIGAERO-CIMS, hereafter CIMS; Aerodyne Research Inc., Billerica, MA, USA; Lopez-Hilfiker et al., 2014), were used to measure aerosol composition.

The AMS analyses the chemical composition of incoming aerosol particles up to 1 µm in diameter in real-time. The non-refractory particles are flash vaporised at 600 °C on the impact of a tungsten surface and the resulting vapour is fragmented and ionised by electron impact ionisation (70 eV) before reaching the entrance of the time-of-flight region, after which the fragmented ions are detected using a multi-channel plate (MCP) detector. The AMS is able to provide a quantitative time series of organic aerosol, nitrate, sulfate, ammonium and chloride, in addition to high-resolution information about the elemental composition of ion fragments. The ionisation efficiency (IE) for nitrate was determined from a series of calibrations carried out before and after this campaign. The relative ionisation efficiency (RIE) for sulfate was determined from calibration carried out post-campaign. The RIE for organic aerosols and MSA were taken from standard literature values: 1.4 for organic aerosol (Canagaratna et al., 2007; Nault et al., 2023) and 1.3 for MSA (Zorn et al., 2008).

The CIMS uses iodide-adduct ionisation, a soft ionisation method that limits analyte fragmentation, thereby facilitating the identification of individual compounds. The iodide reagent is generated by passing N_2 over a permeation tube containing methyl iodide, then ionised using an X-ray source. During this campaign, the CIMS was used with a FIGAERO inlet, designed for online sampling of ambient air, with the gas and particle phases sampled separately via two dedicated ports. For the analysis of the particle phase, particles were first collected on a 25 mm PTFE filter for fifty minutes. When the collection was complete, an actuator moved the filter into position in front of the inlet. Heated nitrogen was passed through the filter, vaporising the sample. The temperature of the nitrogen was increased from room temperature to 200 °C over 20 minutes, allowing the separation of species based on volatility. Filter samples were collected and analysed *in situ* with a time resolution of two hours (one hour of sampling followed by one hour of heating and cooling cycle). Air was sampled via the laboratory's main inlet, which has an aerodynamic diameter cutoff of 10 µm.

Data analysis for the AMS was carried out using the standard AMS analysis software (SQUIRREL v1.66G and PIKA v1.26G). Analysis of the CIMS data was carried out using TofWare version 4.0.2. The signal of each fitted peak was normalised to 10^6 counts per second (cps) of the reagent ion iodide. For each peak, the time series over the heating cycle – known as a thermogram – was integrated, providing a single value for the signal for each fitted peak per filter collection.

Data was collected using the AMS between 13 January and 18 February 2023. Online measurements of the gas- and particle-phase composition were carried out using the CIMS between 7 and 18 February 2023. During the campaign, aerosol sampling was carried out via the observatory's 15 m inlet (20 cm inner diameter (ID)), which draws 300 L min^{-1} of air from the top of the MCOH tower (Corrigan et al., 2006). Individual instruments sampled directly from this main inlet. For the AMS, air was

https://doi.org/10.5194/egusphere-2026-914
Preprint. Discussion started: 11 March 2026

drawn through stainless steel tubing (1/4-inch outer diameter (OD)) via a dryer before entering the instrument. After 25 January, the instrument switched between three different sampling modes (V mode (lower mass resolution; greater mass range; greater sensitivity), W mode (higher mass resolution; smaller mass range; lower sensitivity) and soot particle (SP) mode (in which an intracavity laser vaporiser is switched on to enhance detection of refractory particles (Onasch et al., 2012)) over 15 minutes. However, only data from V mode with the SP laser off are presented here. Once per day, zero data to be used as a blank was collected for 10 minutes by pulling lab air into the AMS through a HEPA filter. The collection efficiency (CE) used for this dataset was 0.45, as suggested by Middlebrook et al. (2012) for particles that are not acidic and do not contain large amounts of nitrate. To justify these assumptions, an ion balance was carried out to establish the ratio of measured NH_4 to the NH_4 that would be required to neutralise the observed anions. This ratio was found to be 1.01; the close proximity to unity suggests that the observed aerosol was neutral (see Text S1). Nitrate made up only 1.4% of the aerosol mass detected by the AMS, indicating that the assumption of low nitrate concentrations is also justified in this case.

Humidity, temperature and rainfall were monitored using a Vaisala Weather Transmitter (WXT520), which recorded with a time resolution of three minutes. The inlet for ambient air collection at MCOH was positioned at the top of a 15 m-tall tower that reached above the treeline. Information on wind speed and direction during the campaign was provided with 10-minute time resolution from Hanimaadhoo Airport, 3 km southwest of the measurement site. These data were provided by the Maldives Meteorological Service (MMS).

2.4 CIMS calibration of MSA and ammonium sulfate

Sensitivity calibrations of MSA and ammonium sulfate (AS) were performed using the X-Ray ionising source to obtain calibration curves for the CIMS. The resulting calibration curves are shown in Figure S1.

To achieve these, the calibration compound was dissolved in MilliQ water and nebulised. The particle stream was then directed through a dryer with silica gel before reaching a Differential Mobility Analyser (DMA) for size selection. The monodisperse aerosol was simultaneously directed to a Condensation Particle Counter (CPC) and the FIGAERO inlet, where it was collected on a pre-baked filter. The same heating sequence was used for the calibration filters as for the sample filters (20 min heating to 200 °C, 20 min soaking and 20 min cooling). As zero points for the calibration curves, pure MilliQ water was collected for 10 minutes. For the MSA, signal strength was determined from the CH_4SO_3-I peak at *m/z* 223. Ammonium sulfate is not detected by the CIMS as NH_4SO_4 adducted with iodide, but rather, contributes towards a series of peaks representing inorganic clusters including HSO_4^-, SO_3-I^- and H_2SO_4-I^-, as well as several others. During calibration, the SO_3-I peak at *m/z* 207 was found to be the most stable, and was therefore used in the calibration of AS.

A line was fitted to the calibration points for both MSA and AS and the equation of the straight line was calculated, with the line forced through zero (Fig. S1). The slope of the line was used to convert the signal strength unit to mass, based on the sample peaks of CH_4SO_3-I and SO_3-I. That mass was then converted to a mass concentration by accounting for the flow rate and the sampling collection time. During the field campaign, it is plausible that other parent molecules, in addition to AS, may

https://doi.org/10.5194/egusphere-2026-914
Preprint. Discussion started: 11 March 2026

have contributed towards the fragment at SO_3-I. The calculated concentrations of AS presented from CIMS measurements here are therefore to be considered an upper bound.

3 Results

3.1 Meteorological conditions

The observed wind originated almost exclusively from between 330° and 90° (NNW to E) (Fig. 1b). This was generally consistent throughout the campaign, with the largest fluctuations in the days immediately following a rainfall event that occurred on the evening of 23 January, and again between 4 and 7 February. The average observed wind speed was 2.84 m s^{-1}, with a standard error (hereafter shown after ±) of 0.02 m s^{-1}, and a standard deviation (std) of 1.14 m s^{-1}. The strongest winds occurred during the night of 23 January, peaking at 7.87 m s^{-1}. Temperature and relative humidity (RH) remained relatively consistent throughout the campaign. The average temperature was 27.33 ± 0.01 (std 0.89) °C and RH was 72.44 ± 0.05 (std 6.18) %. This is consistent with the typical conditions at this site at this time of year (Budhavant et al., 2018, 2024; Ramachandran and Rupakheti, 2020).

For analysis, three time periods were selected to represent different air mass back trajectories. These are marked out in Fig. 1a. Each time period is four days long, with period 1 covering 15–19 January (08:00–08:00 local time (MVT)), period 2 covering 30 January–3 February (09:00–09:00 MVT) and period 3 covering 14–18 February (06:00–06:00 MVT). During periods 1 and 3, the wind direction originated primarily from the east, while northerly winds characterised period 2. The cluster mean of hourly generated ten-day back trajectories for each period, along with fire counts for the period from 12 January to 18 February 2023, are shown in Fig. 1c. Here, it can be seen that the air mass sampled during period 1 originates from the Bay of Bengal and southern and north-east India, while during period 2 the air mass originated from western India and Pakistan, with a large amount of time spent over the Arabian Sea. Period 3 represents a mixture of trajectories from both origins; however, it has a cluster mean very similar to period 1. The fire counts show that fires influence air masses originating from all three back trajectories. All generated back trajectories for each period are shown in Figure S2. These periods are used to analyse the influence of the source region on aerosol composition.

https://doi.org/10.5194/egusphere-2026-914
Preprint. Discussion started: 11 March 2026

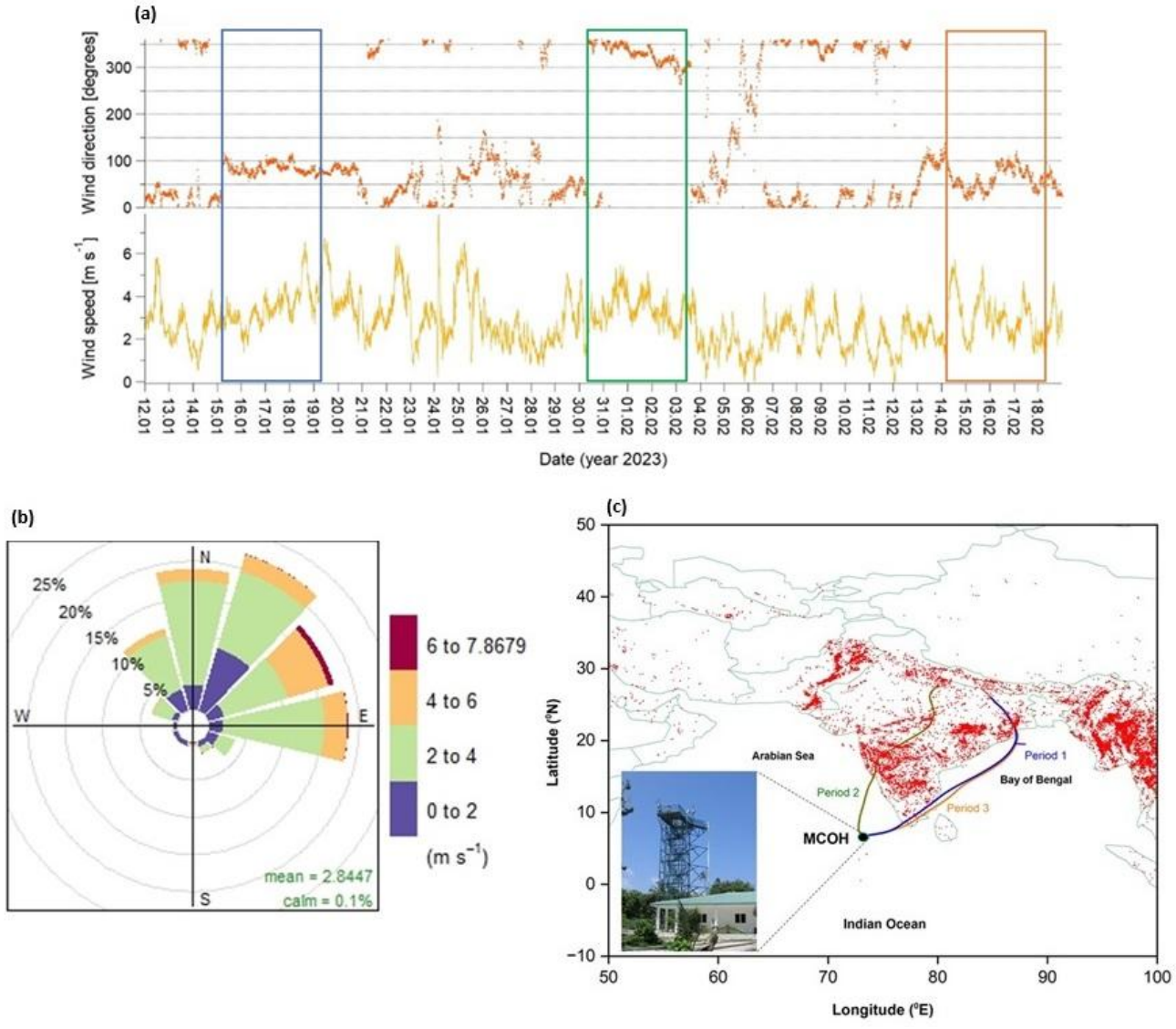

Figure 1: (a) Time series of wind speed and direction observed during the campaign, with the three time periods marked out in blue (period 1), green (period 2) and orange (period 3). (b) Wind rose summarising wind speed and direction at Hanimaadhoo Airport from 12 January 2023 to 18 February (c) Cluster mean of 10-day back trajectories during the outlined periods. Fire count data from 12 January to 18 February 2023 is marked as red dots.

3.2 Aerosol chemical composition

Sulfate provided the largest contribution to non-refractory PM_1 mass across all three time periods. The contribution of sulfate, nitrate, chloride, ammonium and organic mass observed by the AMS during each time period and averaged over the field campaign as a whole is shown in the bar graph in Fig. 2a. Sulfate represented 51.8% of the total non-refractory PM_1 mass loading, followed by organic aerosol (26.2%) and ammonium (20.2%), with a small contribution from nitrate and chloride.

https://doi.org/10.5194/egusphere-2026-914
Preprint. Discussion started: 11 March 2026

The average mass concentration of sulfate species during the campaign period was 6.49 ± 0.02 (std 3.07) μgm^{-3}. The organic and ammonium species average mass concentrations were 3.29 ± 0.01 (std 1.39) and 2.54 ± 0.01 (std 1.12) μgm^{-3} respectively, while the nitrate average was 0.18 (std 0.08) μgm^{-3} and the chloride 0.04 (std 0.03) μgm^{-3}.

The time series of each species' mass concentration over the campaign period is shown in Fig. 2c, with the three time periods highlighted. There were variations in the total aerosol mass loading throughout the campaign, most notably after a rainfall event on 23 January, when aerosol mass reduced substantially. The concentration of sulfate increased across the three time periods, with the highest relative and absolute concentration observed during period 3. The largest difference in sulfate contribution was seen between periods 1 and 3, which originated largely from similar source regions. These variations in mass loading did not, therefore, appear to be strongly linked to air mass origin.

The chemical composition of organic aerosol, observed by the AMS, is indicative of low-volatility, oxygenated organic aerosol (LV-OOA). The average contribution of *m/z* 44 to the full organic mass spectrum (f_{44}), which typically represents the fragment CO_2^+ in ambient data and is used as a proxy measurement for more oxidised aerosol, was 0.24 (std 0.02), leading to the estimated average oxygen-to-carbon (O:C) ratio of 1.11 (std 0.12). This suggests an aerosol mass that has been exposed to substantial oxidation and ageing (Ng et al., 2011). The elemental composition of the organic aerosol was remarkably similar across the three highlighted time periods as seen in Fig. 2b, indicating that this is basically independent of air mass origin. This is also indicated by the mass spectra for all three time periods, shown in Figure S3, which show little to no variation between the different time periods for all species.

Nitrate contributed only 1.45% to the total PM_1 mass observed by the AMS. However, high concentrations of nitric acid (HNO_3I^-) were detected in the PM_{10} by the CIMS, which is often considered to be an indication of the presence of inorganic nitrate (Ye et al., 2021). This suggests that inorganic nitrate was likely present, but only in the coarse mode. Previous research has found that it is common for nitrate to be lost from fine mode aerosol during transport as a result of dilution, with ammonium nitrate salts (NH_4NO_3) dissociating and HNO_3 being emitted in its gaseous form. This HNO_3 is then taken up by coarse mode sea salt aerosol, for example by displacing the chlorine in sodium chloride (NaCl) to produce sodium nitrate ($NaNO_3$). In effect, this leads to the gradual transfer of nitrate from the fine mode into the coarse mode (Yeatman et al., 2001). A similar phenomenon, with nitrate absent in the AMS spectrum while HNO_3-I^- is detected in the particle phase by the CIMS, has been observed using a similar instrumental configuration over the Central Arctic Ocean (Siegel et al., 2023). This observation is therefore consistent with the air mass having been transported over the ocean for an extended period.

It has previously been demonstrated in the AMS that the ratio between the observed fragments of NO^+ at *m/z* 30 and NO_2^+ at *m/z* 46 can be used to estimate whether the nitrate signal is predominantly the result of inorganic NH_4NO_3 or of organonitrates, with the ratio being much higher when the signal originates from organonitrates (Farmer et al., 2010). Here, we observed an NO^+:NO_2^+ ratio of 5.16. This is substantially higher than would be expected from NH_4NO_3, which typically produces ratios of around 2 for our instrument. This suggests that the small amount of nitrate observed in the fine mode aerosol after transport is organic in nature.

https://doi.org/10.5194/egusphere-2026-914
Preprint. Discussion started: 11 March 2026

The high sulfate contribution is consistent with previous measurements at the site and has been primarily attributed to secondary sulfate aerosol formed from anthropogenic SO_2 during long-range transport from the continent (eg Clarke et al., 2025). Ship emissions from ocean traffic over the northern Indian Ocean may contribute to the sulfate observed at MCOH (Budhavant et al., 2024), although this influence is likely to have reduced as a result of the introduction in 2020 of IMO2020 regulations requiring ships to reduce sulfur emissions (Sáez Álvarez, 2021). In addition, there are natural sources for the sulfate, for example the small contribution from MSA formed by DMS oxidation. Emissions of hydrogen sulfide (H_2S) released from the large mangrove forest area in Bangladesh (Ganguly et al., 2018), which becomes oxidised to SO_2 in the gas phase and then contributes to the formation of sulfate aerosol, are also a possible source for sulfate that ends up at the MCOH site.

These observations – both the relative stability of the aerosol chemical composition across source regions and the composition itself – indicate that the aerosol observed during this campaign was well-mixed and highly processed, likely as a result of long-range transport. The similarity in composition across source regions, as evidenced by the similar aerosol composition across the three highlighted time periods, suggests that the properties of this aerosol mass are well-mixed and homogeneous across the northern Indian Ocean. These findings are in strong agreement with previous observations at this site during the winter dry season (Budhavant et al., 2018, 2024; Spencer et al., 2008), suggesting that the observations presented here are broadly representative of this site and season.

https://doi.org/10.5194/egusphere-2026-914
Preprint. Discussion started: 11 March 2026

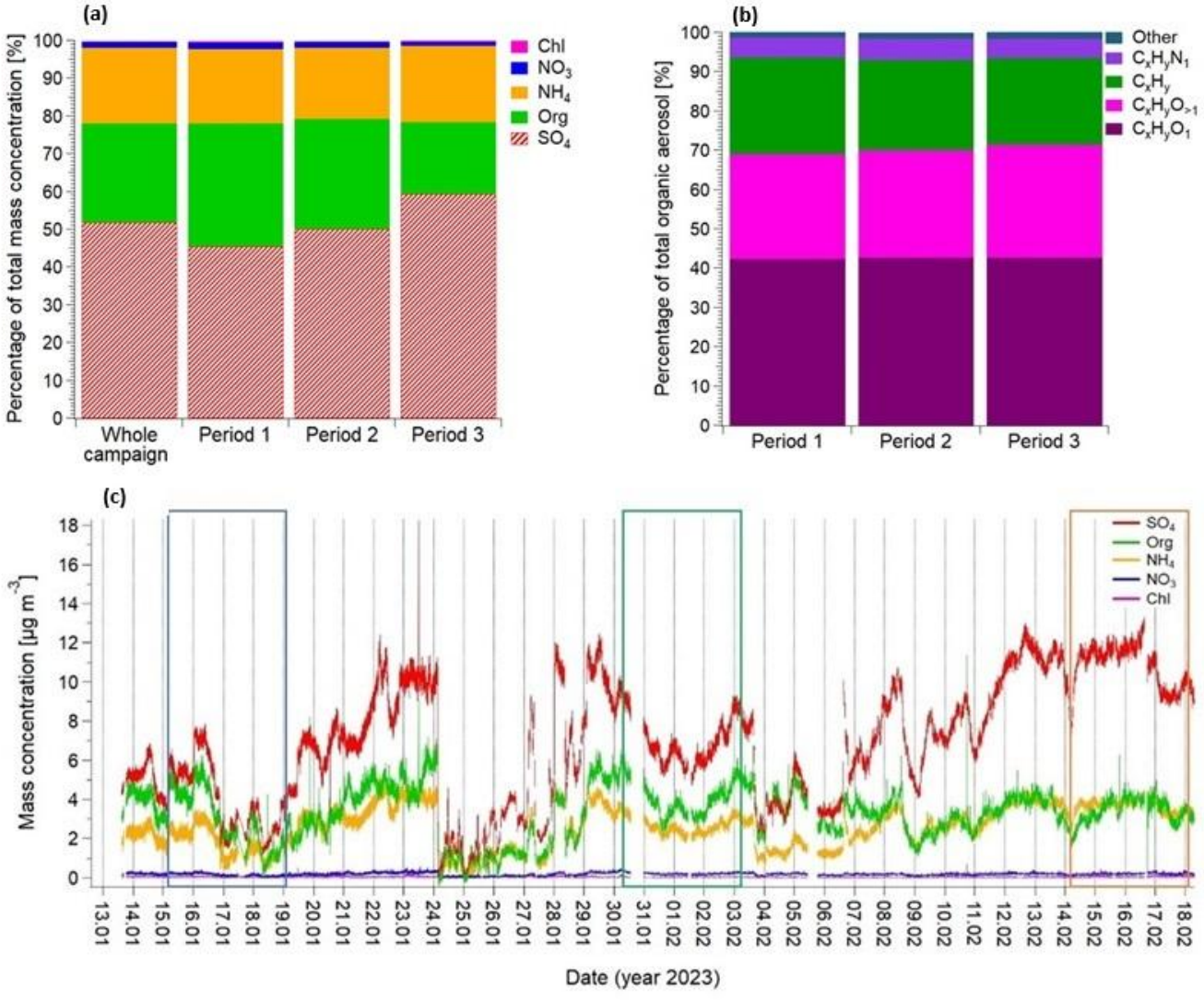

Figure 2: (a) Percentage of the total mass concentration that each species, observed with the AMS, makes up over the whole campaign period as well as over the three chosen time periods. (b) Percentage of the total organic signal measured with the AMS that different elemental compositions make up over the three time periods. (c) Time series of the mass concentration of each species observed with the AMS during the campaign, with the three time periods marked out in blue (period 1), green (period 2) and orange (period 3).

265

3.3 Sulfate aerosol characterisation

As stated in the previous section, sulfate was the most abundant species detected by the AMS at MCOH, with an average mass concentration of 6.49 ± 0.02 µgm^{-3} over the whole campaign period. Previously reported sulfate average mass concentration at the site by Nair et al. (2024), using high-volume samplers and ion chromatography to analyse water-soluble inorganic

https://doi.org/10.5194/egusphere-2026-914
Preprint. Discussion started: 11 March 2026

components, during December to February was 11 (std 6) µg m^{-3}, of which 98% was estimated to be non-sea-salt sulfate. While this is slightly higher than the concentration reported here, the two values are comparable. The AMS samples PM_1 aerosol while Nair et al. (2024) sampled $PM_{2.5}$ (aerosol with a diameter smaller than 2.5 µm), which may explain the lower magnitude in our observations. Previous studies have found that the majority of non-sea-salt sulfate at MCOH is inorganic and originates from an anthropogenic source (Budhavant et al., 2024; Clarke et al., 2025; Spencer et al., 2008).

The analysed sulfate data from the AMS and CIMS both agree with previous research that sulfate is mostly inorganic. The timeseries for the AMS and CIMS sulfate mass concentration are shown in Figure S4. The relative strength of the signal fragments at $H_2SO_4^+$ (f_{H2SO4}) and HSO_3^+ (f_{HSO3}) in the AMS mass spectrum has previously been shown to indicate the relative contribution of ammonium sulfate (AS), methanesulfonic acid (MSA), organosulfurs (OS) and sodium sulfate (SS) towards the total AMS sulfate signal (Chen et al., 2019). In this dataset, the high contribution of f_{H2SO4} to the sulfate signal (Figure S5) indicates the clear dominance of AS. This is also suggested by a rough ion balance estimate, where the measured ammonium fully neutralises the measured sulfate, nitrate and chloride (Zhang et al., 2007, Text S1). The dominance of inorganic sulfate is supported by the average mass spectrum from the CIMS particle phase measurements, which was dominated by inorganic sulfate clusters and compounds (Fig. 3).

The concentration of MSA can be estimated from the AMS data using the $CH_3SO_2^+$ fragment observed at *m/z* 79 (Hodshire et al., 2019). These results indicate that MSA was present throughout the campaign but accounted for only a tiny fraction of the overall SCO. The CIMS data can validate these results using the iodide-MSA adduct ($ICH_4SO_3^-$) observed at *m/z* 223, which is also present, but only in small amounts. A time series of the MSA mass concentration from both AMS and CIMS data is shown in Figure S6. Using the derived MSA mass concentration from AMS measurements, we can estimate that the average concentration of MSA during the campaign was 10.1 ± 0.1 (std 3.9) ng m^{-3}. The mass ratio of MSA to sulfate during the campaign was therefore 0.15%.

https://doi.org/10.5194/egusphere-2026-914
Preprint. Discussion started: 11 March 2026

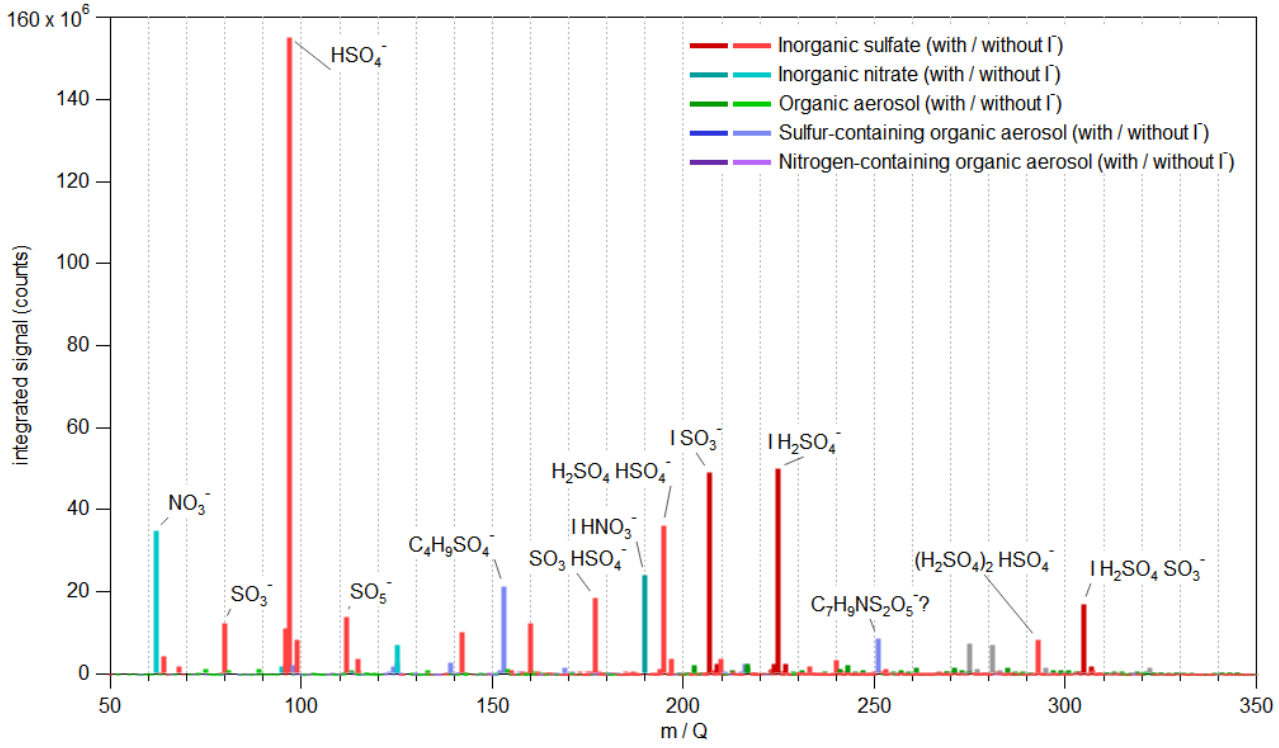

Figure 3: The average background-subtracted CIMS mass spectrum from integrated thermograms. Different classes of compound are shown in different colours. The majority of large peaks in the mass spectrum are from inorganic sulfate peaks.

3.4 Sulfur-containing organic aerosol

During the campaign, 18 SCO species were identified with a clear signal in the online CIMS mass spectrum. Example peak fits for six of these compounds are shown in Fig. 4, and the remaining peak fits are displayed in the supplementary materials in Figure S7. The molecular formulae for all 18 SCOs are listed in Table 1, alongside potential sources based on results from previous studies. Almost all of these compounds were observed as ions assumed to have formed from deprotonation, not as adducts with iodide. Ionisation of SCOs by hydrogen removal is likely to occur with the soft ionisation technique employed by the CIMS when using Iodide as the reagent. In all cases, the observed anion is presented, not the neutral compound. Of the identified SCOs, six have been previously identified at the site (Stone et al., 2012), and nine have been previously associated with isoprene as a precursor (Stone et al., 2012; Wang et al., 2021). Two have previously been associated with aromatic or polycyclic aromatic (PAH) oxidation (Le Breton et al., 2019; Riva et al., 2015). There was no evidence of SCOs associated with monoterpene or sesquiterpene precursors.

The largest SCO signal by a large margin was $C_4H_9O_4S^-$, observed at *m/z* 153, which was also observed clustered with the iodide reagent ion as $IC_4H_{10}O_4S^-$ at *m/z* 281. This compound has not been reported in previous studies, including those focused on SCOs at this field site (Stone et al., 2012). The source of this large signal is therefore unclear. It is plausible that this

https://doi.org/10.5194/egusphere-2026-914
Preprint. Discussion started: 11 March 2026

compound could be the result of a reaction between ethanol – a common pollutant in urban air (eg Li et al., 2022) – and sulfuric acid (Japar et al., 1990). However, this product has not been reported in the atmosphere before.

Our observations are consistent with previous suggestions that the majority of these SCOs are formed when biogenic VOCs – particularly isoprene – interact with inorganic sulfate aerosol during transport (Stone et al., 2012). Isoprene is emitted in considerable amounts by the biosphere. While most of it is emitted by terrestrial vegetation, there is also a minor marine biogenic source (Conte et al., 2020). It should be noted that while $C_4H_7O_5S^-$ and $C_4H_7O_6S^-$ have been reported in previous studies to be associated with the oxidation of isoprene in the presence of sulfate (Wang et al., 2021), the same molecular formulae have also been identified in FIGAERO-CIMS measurements in Beijing, where they were connected to the heterogeneous chemistry between anthropogenic VOCs and sulfate (Le Breton et al., 2018). It remains challenging to pinpoint the precursors of the SCOs observed at MCOH.

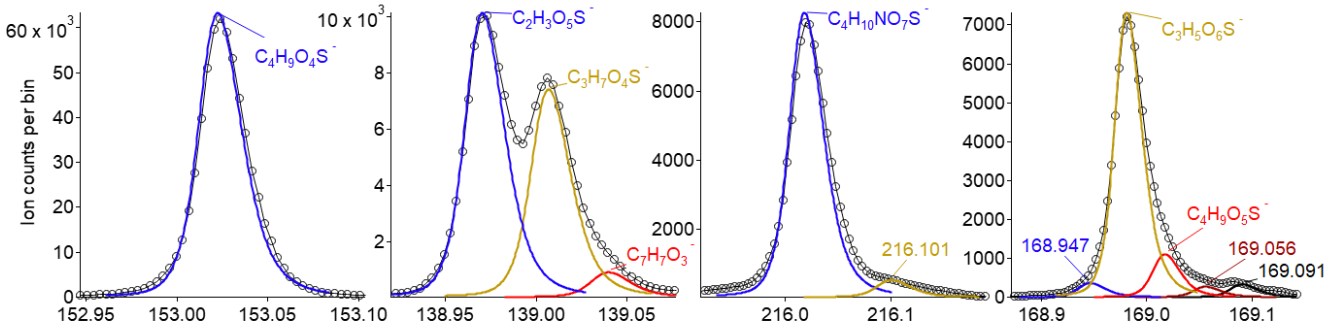

Figure 4: Peak fits for six of the larger sulfate signals observed by the CIMS.

Table 1: Observed SCOs, listed in order of signal size.

Molecular formula	*m/z*	Potential compound	Potential source	Citations
$C_4H_9O_4S^-$ (also detected as $C_4H_{10}O_4S\text{-}I^-$)	153 (281)	Diethyl sulfate		
$C_2H_3O_5S^-$	139	Sulfoacetic acid / acetoxysulfonic acid	Isoprene	Stone et al., 2012; Hansen et al., 2014
$C_4H_{10}NO_7S^-$	216			
$C_3H_5O_6S^-$	169	Sulfolactic acid	Isoprene, lactic acid	Stone et al., 2012; Le Breton et al., 2018
$C_3H_7O_6S^-$	171	Glycerol sulfate	Isoprene	
$C_3H_7O_4S^-$	139	Hydroxypropanesulfonic acid		
$C_5H_{11}O_7S^-$	215	Pentaerythritol sulfate	Isoprene, IEPOX	Stone et al., 2012;

https://doi.org/10.5194/egusphere-2026-914
Preprint. Discussion started: 11 March 2026

				Le Breton et al., 2018
$C_4H_3O_8S^-$	211			
$C_2H_3O_6S^-$	155	GAS	Isoprene, glycolic acid	Stone et al., 2012; Le Breton et al., 2018
$C_4H_9O_5S^-$	169			
$C_5H_{11}O_6S^-$	199			Wang et al., 2021
$C_4H_7O_5S^-$	167		Aromatics, isoprene	Hansen et al., 2014; Wang et al., 2021; Le Breton et al., 2018
$C_5H_7O_7S^-$	211			Stone et al., 2012
$C_4H_7O_6S^-$	183		Benzene, isoprene	Stone et al., 2012; Wang et al., 2021
$C_4H_7O_7S^-$	199		Isoprene	Le Breton et al., 2018; Wang et al., 2021
$C_4H_9O_7S^-$	201			
$C_5H_9O_5S^-$	181			Wang et al., 2021
$C_4H_7O_4S^-$	151			Wang et al., 2021

3.5 Organic aerosol chemical composition

The organic aerosol was primarily made up of organic acids and dicarboxylic acids. A list of 25 identified organic molecular formulae, which make up 61% of the total CHO signal, is provided in Table 2, together with their potential compound name and source. Of the identified CHO compounds, 27% of the signal by mass was made up by dicarboxylic acids, which are common components of organic aerosol.

The highest measured signal was identified as oxalic acid. Oxalic acid has many identified sources, such as fossil fuel combustion, biomass burning and biogenic emissions. However, several studies have shown that primary emissions of oxalic acid are insufficient in explaining the high concentrations of oxalic acid measured in the atmosphere. Indeed, a large fraction of particulate oxalic acid (or oxalate, the anion of oxalic acid) is actually secondary, formed through chemical cloud processing of aerosols (Ervens et al., 2011; Sorooshian et al., 2006). The high concentrations of oxalic acid therefore, indicate that cloud processing likely shapes the physicochemical properties of aerosol particles transported to MCOH. This is also visible in previously published aerosol number size distribution data from the site, which shows a bimodal size distribution (Budhavant et al., 2018) characteristic of aerosol populations that have undergone chemical cloud processing (Feingold and Kreidenweis, 2000; Hoppel et al., 1994).

https://doi.org/10.5194/egusphere-2026-914
Preprint. Discussion started: 11 March 2026

Table 2: Observed particle-phase CHOs, listed in order of signal size. Each of these compounds was detected as an adduct to the iodide regent anion (I-).

Molecular formula	Potential compound	Likely compound family	Potential source	Citations
$C_2H_2O_4\,I^-$	oxalic acid	dicarboxylic acid	photochemistry; in-cloud processing; biomass burning; vehicular exhaust	Hsieh et al., 2007;Meng et al., 2014; Xu et al., 2020; Yu et al., 2005
$C_4H_4O_4\,I^-$	fumaric acid / maleic acid	dicarboxylic acid	anthropogenic sources; vehicular exhaust; oxidation of aromatic compounds	Kawamura and Kaplan, 1987; Röhrl and Lammel, 2002; Sato et al., 2021
$C_2H_4O_3\,I^-$	glycolic acid	organic acid	biogenic sources; oxidation of vehicular exhaust	Le Breton et al., 2019; Souza et al., 1999
$C_6H_6O_5\,I^-$			biomass burning; oxidation of aromatic compounds	Nakao et al., 2011; Yee et al., 2013
$C_5H_4O_5\,I^-$		organic acid	oxidation of aromatic compounds	Li et al., 2021
$C_4H_6O_5\,I^-$	malic acid	dicarboxylic acid	isoprene oxidation; biogenic sources	Massoli et al., 2018; Nguyen et al., 2010; Röhrl and Lammel, 2002
$C_3H_6O_3\,I^-$	lactic acid / hydroxypropionic acid / peroxypropionic acid	organic acid	isoprene oxidation; cooking emissions; oxidation of vehicular exhaust	Le Breton et al., 2019; Nguyen et al., 2011; Reyes-Villegas et al., 2018
$C_4H_2O_4\,I^-$	acetylenedicarboxylic acid	dicarboxylic acid	oxidation of aromatic compounds (furan)	Chen et al., 2022
$C_5H_6O_5\,I^-$		ketone	aqueous processing of biomass burning emissions; oxidation of vehicle	Massoli et al., 2018; Mehra et al., 2020; Zhao et al., 2014

https://doi.org/10.5194/egusphere-2026-914
Preprint. Discussion started: 11 March 2026

			emissions; oxidation of biogenic compounds	
$C_3H_4O_5\ I^-$			isoprene oxidation; oxidation of aromatic compounds	Chen et al., 2020; Cheng et al., 2024
$C_5H_6O_4\ I^-$		dicarboxylic acid	oxidation of aromatic compounds; biomass burning; isoprene oxidation	Nguyen et al., 2011; Oghama et al., 2025; Praplan et al., 2014
$C_5H_4O_2\ I^-$	furfural	aldehyde	biomass burning; anthropogenic sources	Romanias et al., 2024
$C_6H_6O_6\ I^-$			oxidation of aromatic compounds	Mehra et al., 2020
$C_3H_4O_4\ I^-$	malonic acid / hydroxypyruvic acid	dicarboxylic acid	photochemistry; oxidation of aromatic compounds; vehicular emissions	Hsieh et al., 2007; Yao et al., 2004
$C_7H_8O_5\ I^-$	pentahydroxy toluene		biomass burning; oxidation of aromatic compounds	Schwantes et al., 2017; Yee et al., 2013
$C_7H_6O_5\ I^-$		phenolic	biomass burning; oxidation of aromatic compounds	Yee et al., 2013
$C_6H_8O_4\ I^-$			isoprene oxidation	Nguyen et al., 2011; Yee et al., 2013
$C_5H_8O_4\ I^-$	glutaric acid / methylsuccinic acid	dicarboxylic acid	isoprene oxidation; vehicle exhaust	D'Ambro et al., 2017; Kawamura and Kaplan, 1987
$C_5H_8O_5\ I^-$	hydroxyglutaric acid	organic acid	isoprene oxidation; monoterpene oxidation	Chen et al., 2020; Kleindienst et al., 2007
$C_6H_6O_4\ I^-$	muconic acid	dicarboxylic acid	biomass burning; oxidation of aromatic compounds	Yee et al., 2013
$C_3H_2O_4\ I^-$		organic acid	photochemistry	Boris et al., 2014; Gallimore et al., 2011
$C_6H_8O_6\ I^-$			oxidation of aromatic compounds (phenol)	Nakao et al., 2011

https://doi.org/10.5194/egusphere-2026-914
Preprint. Discussion started: 11 March 2026

$C_7H_8O_6\,I^-$		oxidation of aromatic compounds	Mackenzie-Rae et al., 2018; Mehra et al., 2020
$C_9H_4O_5\,I^-$		oxidation of polycyclic aromatic hydrocarbons (PAHs)	Oh et al., 2022
$C_6H_6O_2\,I^-$	catechol	biomass burning	Adounkpe et al., 2013; Veres et al., 2010

3.6 Transport of continental emissions and comparison with CIMS measurements from Delhi

The HYSPLIT back trajectories indicate that the Indian sub-continent was an important source region for aerosol observed at MCOH during this campaign. This is supported by previous research carried out at the site (e.g., Dasari et al., 2025). Here, we compare the characteristics of organic aerosol observed at MCOH with that of organic aerosol observed using the CIMS during a campaign in Delhi in 2019 (Haslett et al., 2023; Mishra et al., 2023), which is used as an illustrative example of the chemical composition in the source region. This provides some insight into the impact of processing and transport on aerosol chemical characteristics.

Biomass burning provides the largest contribution towards the organic spectrum observed in Delhi. This is evidenced by levoglucosan, a marker of fresh biomass burning, being the dominant CHO compound observed in Delhi. Its contribution to the total signal from CHO and CHON species in Delhi is evident in the O:C plot displayed in Fig. 5b, where the large bar corresponds to compounds with 6 carbon and 5 oxygen atoms. This is made up almost entirely by the signal at $C_6H_{10}O_5$, which comes from levoglucosan and other anhydrous sugars released from biomass burning. Levoglucosan is degraded during atmospheric transport (Li et al., 2021a) and does not therefore dominate the spectrum at MCOH in the same way, although it was present in small quantities in the CIMS mass spectrum. Nevertheless, as is detailed in Table 2, several observed organic species indicate either the unambiguous influence of biomass burning aerosol (eg catechol) or the oxidation of aromatic compounds, which could have been emitted from a number of sources including biomass burning. Although levoglucosan is typically considered the most unambiguous marker of biomass burning's influence on an air mass, its short lifetime during transport makes it less suitable for identifying sources of aerosol transported over large distances. Results presented here indicate that exploring the stability and degradation of other compounds associated with biomass burning may prove more beneficial in identifying its influence on more highly-processed aerosol.

The substantial contribution of CHON compounds to the total CIMS signal in Delhi – representing just under 30% of the total CHO and CHON signal – suggests oxidation chemistry taking place in a high-NO_x environment, as a result of emissions from traffic and biomass burning. In contrast, by the time the polluted air mass arrives at the receptor site at MCOH, CHON compounds contribute only 9% towards the total CHO + CHON signal. Chamber experiments have previously demonstrated

https://doi.org/10.5194/egusphere-2026-914
Preprint. Discussion started: 11 March 2026

that CHON compounds are likely to be removed from the particle phase during transport under ambient conditions as a result of hydrolysis, with atmospheric lifetimes of hours to days (Bean and Hildebrandt Ruiz, 2016; Liu et al., 2012). The reduction in the contribution of CHON at MCOH after transport strongly supports this hypothesis.

In the source region in Delhi (Fig. 5b and d), a high number of different organic compounds were identified, including many with longer chain lengths of 12–20 carbon atoms. This suggests the influence of a complex mix of sources that has undergone limited processing. When the air mass reached MCOH (Fig. 5a and c), there were fewer identified compounds, with a higher total ratio of oxygen atoms per carbon. The chain lengths were shorter, and the majority of the signal was made up of simple dicarboxylic acids and other organic acids. This suggests more processed and more oxidised aerosol. These small molecules could also be associated with aqueous phase chemistry, suggesting the influence of cloud processing.

Although characterisations of organic aerosol in southern India are scarce, existing measurements indicate that here, too, the organic fraction is dominated by oxalic acid, which, during the winter season, is largely produced from the photo-oxidation of biogenic and anthropogenic VOCs (Hegde et al., 2016). This, together with the limited variation in relative chemical composition at MCOH during this campaign, regardless of air mass back trajectory, suggests that aged and processed aerosol from the more polluted north may already be among the dominant sources of pollution when the air mass passes over southern India.

The air masses intercepted at MCOH had spent considerable time over the ocean prior to sampling. For those originating from the east, which travelled over the Bay of Bengal and southern India, the air masses were over the ocean for between 1 and 3 days after leaving the continent. Those originating from the north were transported across the marine environment for 4-6 days. It is possible that aerosol composition could have been influenced by deposition and new formation in addition to photolysis and aqueous processing. More comprehensive measurements in southern India and over the Indian Ocean would be required to more comprehensively identify and quantify these aspects.

https://doi.org/10.5194/egusphere-2026-914
Preprint. Discussion started: 11 March 2026

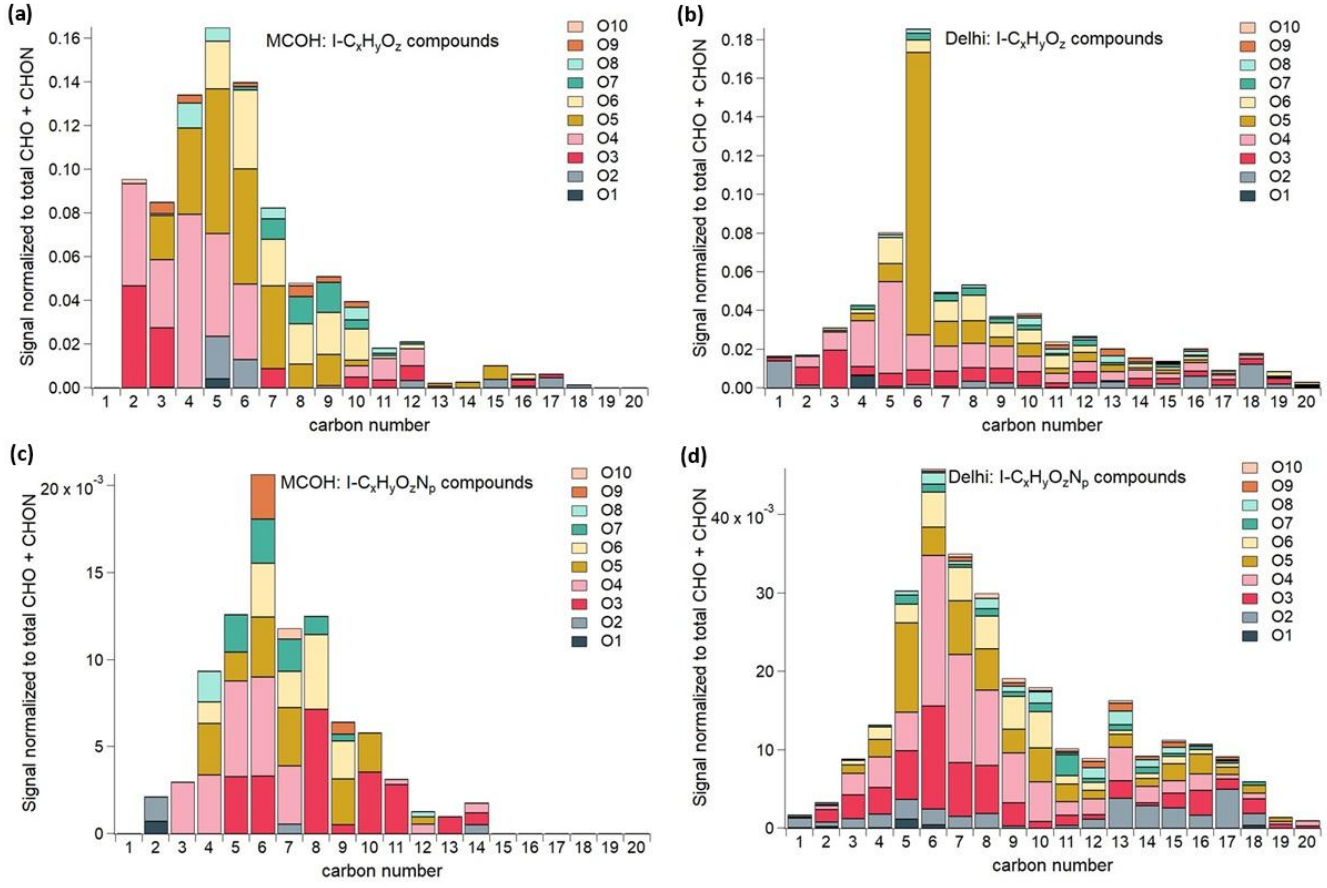

Figure 5: The O:C ratio of identified organic aerosols, where the x-axis shows the carbon number, the colour code the oxygen number and the height of a bar shows the contribution to the total signal of CHO and CHON compounds. Presented for (a) CHO compounds at MCOH, (b) CHO compounds at Delhi, (c) CHON compounds at MCOH and (d) CHON compounds at Delhi.

4 Conclusions

Results presented here show low variability in aerosol chemical composition over the course of this campaign, despite air masses originating from distinct source regions. Although there was an increase in the sulfate-to-organic ratio as the campaign progressed, this did not correlate with air mass source regions. The mass spectra of sulfate and organic compounds remained broadly consistent throughout. This suggests that the regional atmosphere is dominated by well-mixed aerosol that has been aged both photochemically and via cloud processing.

We observed high sulfate mass fractions (on average 52% of non-refractory PM_1), the majority of which was composed of inorganic sulfate, likely formed from anthropogenic SO_2 during transport. Methanesulfonic acid (MSA) was present at a ratio of 0.015 to total sulfate mass. In addition, several SCOs were identified at the site. Some of these have been observed previously

https://doi.org/10.5194/egusphere-2026-914
Preprint. Discussion started: 11 March 2026

at MCOH, but some are reported here for the first time. Surprisingly, the most dominant SCO observed was $C_4H_9O_4S^-$, which may be associated with the compound diethyl sulfate. To our knowledge, this is the first time this has been identified in the ambient atmosphere. Overall, the composition of observed SCOs suggests formation from the reaction of both biogenic and anthropogenic VOCs with inorganic sulfate during transport.

Dicarboxylic acids and other organic acids made up the majority of the signal for CHO compounds. Their dominance indicates highly-aged aerosol that could have originated from a variety of sources, both biogenic and anthropogenic. In comparison with mass spectra observed in the city of Delhi, which is taken to be representative of one of the key source regions for observed air masses, we found higher O:C ratios, shorter chain lengths and fewer distinct compounds at MCOH. While levoglucosan – which is indicative of fresh biomass burning – dominated the spectrum in Delhi, its signal was barely observed at MCOH as a result of degradation during transport. Similarly, the high CHON signal observed in Delhi was not seen at MCOH, where the organic signal was dominated by CHO compounds.

Results presented here indicate that photochemical and aqueous processing of aerosol during transport is the most important factor governing the chemical composition of aerosol over the Indian Ocean during the winter. The observed mass spectra provide indications of original sources: for example, molecular compositions consistent with catechol and furfural suggest the influence of biomass burning, $C_4H_6O_5$ and $C_3H_4O_5$ suggest the influence of isoprene, and $C_9H_4O_5$ that of polycyclic aromatic hydrocarbons (PAHs), while the composition of various SCOs indicate biogenic and anthropogenic emissions reacting with SO_4 at particle surfaces as a likely source. However, while these insights are valuable for identifying potential sources, the larger part of the observable signal is dominated by inorganic sulfate and organic acids that are, predominantly, an indication of a highly-processed and well-mixed air mass. This is further supported by the similarity in aerosol composition, even in cases where back trajectories indicate different air mass origins.

These findings are consistent with previous studies showing that sulfate and organic compounds dominate non-refractory aerosol mass during the winter at MCOH. Clarke et al. (2025) demonstrated that 94% of sulfate aerosol observed at MCOH is from anthropogenic sources, which is supported by observations of inorganic sulfate aerosol presented here. This is consistent with the interpretation that anthropogenic SO_2 oxidation during transport is a dominant process in its formation. Stone et al. (2012) first characterised SCOs at the MCOH site, identifying a number of distinct compounds. Our results build on this, identifying new compounds and suggesting formation pathways that involve anthropogenic precursors in addition to biogenic. Our results support previous findings showing that biomass burning and fossil fuels are important sources of organic aerosol at MCOH (Sheesley et al., 2011), and that the majority of aerosol observed at the site during the winter is from distant sources (Budhavant et al., 2015). Previous studies have demonstrated changes in aerosol physical properties as a result of aqueous processing during transport (Budhavant, 2018). However, this is the first time that organic aerosol at the site has been characterised on a molecular level, and thus provides the first identification of distinct source markers. Similarly, this is the first time that the strong impact of atmospheric processing on aerosol chemical properties at the molecular level, in addition to physical properties, has been identified at this site.

https://doi.org/10.5194/egusphere-2026-914
Preprint. Discussion started: 11 March 2026

This campaign was time-limited, and therefore provides only a snapshot of aerosol composition at this site. Longer-term observations, in particular across contrasting seasons, would provide more insight into the contribution of different sources at different times of year. Extensive atmospheric processing and the degradation of primary emissions complicates source attribution, so future studies would benefit from measurements across transport pathways, for example using ship-based measurements, to explore the change in aerosol properties during transportation.

Results presented here demonstrate the importance of chemical processing, in additional to physical processing, on aerosol properties over the northern Indian Ocean. A large influence from anthropogenic emissions is clearly indicated by the high inorganic sulfate loading. This highly-processed, sulfate-rich haze will influence aerosol-radiation interactions, in addition to influencing cloud microphysical properties and precipitation patterns. This more comprehensive understanding of the chemical composition and processing of aerosol in this region will improve representation of these processes in atmospheric and climate models. In addition, the identification of molecular source markers presented here indicate how future policy changes could impact air quality in this region.

Data availability.

Data referenced in this study can be accessed via the Bolin Centre Database: https://doi.org/10.17043/haslett-2026-3kux1r-1.

Supplement.

Additional information is available in the supplementary materials.

Author contributions.

This study was conceptualised by KS and SLH. Data collection was carried out by PT, PK, PM, CM, KB and SLH, and data processing and analysis by KS, PT and SLH. Interpretation of results was carried out by KS and SLH, with input from all authors, including substantial input from ASHP, CM, LH and KB. The writing of the manuscript and was carried out by KS and SLH, with editing and contributions from ASHP, CM, LH and KB. Figures were produced by KS, KB and SLH. Funding for field campaigns was acquired by ASHP, SNT, CM and SLH.

Acknowledgements.

The authors acknowledge the support of Örjan Gustafsson (Stockholm University) during the preparation and implementation of the field campaign at MCOH. In addition, we thank the technical staff, Mr. Sharafulla Thoha, Miss. Mariyam, and Mr. Faruhaadh Moosa at MCOH, the Maldives Meteorological Service and the Government of the Republic of Maldives for their support during the field campaign.

https://doi.org/10.5194/egusphere-2026-914
Preprint. Discussion started: 11 March 2026

Financial support.

This work was financially supported by the Swedish Research Council (VR, Grant 2021-05225), the Bolin Centre (under Research Theme 1) and the Polish National Science Center (Grant 2023/49/B/ST10/00513).

Competing interests.

The authors have no competing interests to declare.

5. References

Adounkpe, J., Aina, M., Mama, D., and Sinsin, B.: Gas Chromatography Mass Spectrometry Identification of Labile Radicals Formed during Pyrolysis of Catechool, Hydroquinone, and Phenol through Neutral Pyrolysis Product Mass Analysis, International Scholarly Research Notices, 2013, 930573, https://doi.org/10.1155/2013/930573, 2013.

Aswini, A. R., Hegde, P., Aryasree, S., Girach, I. A., and Nair, P. R.: Continental outflow of anthropogenic aerosols over Arabian Sea and Indian Ocean during wintertime: ICARB-2018 campaign, Science of The Total Environment, 712, 135214, https://doi.org/10.1016/j.scitotenv.2019.135214, 2020.

Bean, J. K. and Hildebrandt Ruiz, L.: Gas–particle partitioning and hydrolysis of organic nitrates formed from the oxidation of α-pinene in environmental chamber experiments, Atmospheric Chemistry and Physics, 16, 2175–2184, https://doi.org/10.5194/acp-16-2175-2016, 2016.

Bharali, C., Nair, V. S., Chutia, L., and Babu, S. S.: Modeling of the Effects of Wintertime Aerosols on Boundary Layer Properties Over the Indo Gangetic Plain, Journal of Geophysical Research: Atmospheres, 124, 4141–4157, https://doi.org/10.1029/2018JD029758, 2019.

Boris, A. J., Desyaterik, Y., and Collett, J. L.: How do components of real cloud water affect aqueous pyruvate oxidation?, Atmospheric Research, 143, 95–106, https://doi.org/10.1016/j.atmosres.2014.02.004, 2014.

Budhavant, K., Bikkina, S., Andersson, A., Asmi, E., Backman, J., Kesti, J., Zahid, H., Satheesh, S. K., and Gustafsson, Ö.: Anthropogenic fine aerosols dominate the wintertime regime over the northern Indian Ocean, Tellus B: Chemical and Physical Meteorology, 70, 1–15, https://doi.org/10.1080/16000889.2018.1464871, 2018.

Budhavant, K., Andersson, A., Holmstrand, H., Satheesh, S. K., and Gustafsson, Ö.: Black carbon aerosols over Indian Ocean have unique source fingerprint and optical characteristics during monsoon season, Proceedings of the National Academy of Sciences, 120, e2210005120, https://doi.org/10.1073/pnas.2210005120, 2023.

Budhavant, K., Manoj, M. R., Nair, H. R. C. R., Gaita, S. M., Holmstrand, H., Salam, A., Muslim, A., Satheesh, S. K., and Gustafsson, Ö.: Changing optical properties of black carbon and brown carbon aerosols during long-range transport from the Indo-Gangetic Plain to the equatorial Indian Ocean, Atmospheric Chemistry and Physics, 24, 11911–11925, https://doi.org/10.5194/acp-24-11911-2024, 2024.

https://doi.org/10.5194/egusphere-2026-914
Preprint. Discussion started: 11 March 2026

Canagaratna, M. r., Jayne, J. t., Jimenez, J. l., Allan, J. d., Alfarra, M. r., Zhang, Q., Onasch, T. b., Drewnick, F., Coe, H., Middlebrook, A., Delia, A., Williams, L. r., Trimborn, A. m., Northway, M. j., DeCarlo, P. f., Kolb, C. e., Davidovits, P., and Worsnop, D. r.: Chemical and microphysical characterization of ambient aerosols with the aerodyne aerosol mass spectrometer, Mass Spectrometry Reviews, 26, 185–222, https://doi.org/10.1002/mas.20115, 2007.

Charlson, R. J., Lovelock, J. E., Andreae, M. O., and Warren, S. G.: Oceanic phytoplankton, atmospheric sulphur, cloud albedo and climate, Nature, 326, 655–661, https://doi.org/10.1038/326655a0, 1987.

Chen, K., Mayorga, R., Raeofy, N., Lum, M., Woods, M., Bahreini, R., Zhang, H., and Lin, Y.-H.: Effects of Nitrate Radical Levels and Pre-Existing Particles on Secondary Brown Carbon Formation from Nighttime Oxidation of Furan, ACS Earth Space Chem., 6, 2709–2721, https://doi.org/10.1021/acsearthspacechem.2c00244, 2022.

Chen, Y., Xu, L., Humphry, T., Hettiyadura, A. P. S., Ovadnevaite, J., Huang, S., Poulain, L., Schroder, J. C., Campuzano-Jost, P., Jimenez, J. L., Herrmann, H., O'Dowd, C., Stone, E. A., and Ng, N. L.: Response of the Aerodyne Aerosol Mass Spectrometer to Inorganic Sulfates and Organosulfur Compounds: Applications in Field and Laboratory Measurements, Environ. Sci. Technol., 53, 5176–5186, https://doi.org/10.1021/acs.est.9b00884, 2019.

Chen, Y., Takeuchi, M., Nah, T., Xu, L., Canagaratna, M. R., Stark, H., Baumann, K., Canonaco, F., Prévôt, A. S. H., Huey, L. G., Weber, R. J., and Ng, N. L.: Chemical characterization of secondary organic aerosol at a rural site in the southeastern US: insights from simultaneous high-resolution time-of-flight aerosol mass spectrometer (HR-ToF-AMS) and FIGAERO chemical ionization mass spectrometer (CIMS) measurements, Atmospheric Chemistry and Physics, 20, 8421–8440, https://doi.org/10.5194/acp-20-8421-2020, 2020.

Cheng, X., Li, Y. J., Zheng, Y., Liao, K., Koenig, T. K., Ge, Y., Zhu, T., Ye, C., Qiu, X., and Chen, Q.: Oxygenated organic molecules produced by low-NO_x photooxidation of aromatic compounds: contributions to secondary organic aerosol and steric hindrance, Atmospheric Chemistry and Physics, 24, 2099–2112, https://doi.org/10.5194/acp-24-2099-2024, 2024.

Clarke, S., Holmstrand, H., Budhavant, K., Remani, M., Haslett, S., Rodiouchkina, K., Kooijman, E., and Gustafsson, Ö.: Isotopic apportionment of sulfate aerosols between natural and anthropogenic sources in the outflow of South Asia, EGUsphere, 1–20, https://doi.org/10.5194/egusphere-2025-5334, 2025.

Conte, L., Szopa, S., Aumont, O., Gros, V., and Bopp, L.: Sources and Sinks of Isoprene in the Global Open Ocean: Simulated Patterns and Emissions to the Atmosphere, Journal of Geophysical Research: Oceans, 125, e2019JC015946, https://doi.org/10.1029/2019JC015946, 2020.

Corrigan, C. E., Ramanathan, V., and Schauer, J. J.: Impact of monsoon transitions on the physical and optical properties of aerosols, Journal of Geophysical Research: Atmospheres, 111, https://doi.org/10.1029/2005JD006370, 2006.

D'Ambro, E. L., Lee, B. H., Liu, J., Shilling, J. E., Gaston, C. J., Lopez-Hilfiker, F. D., Schobesberger, S., Zaveri, R. A., Mohr, C., Lutz, A., Zhang, Z., Gold, A., Surratt, J. D., Rivera-Rios, J. C., Keutsch, F. N., and Thornton, J. A.: Molecular composition and volatility of isoprene photochemical oxidation secondary organic aerosol under

https://doi.org/10.5194/egusphere-2026-914
Preprint. Discussion started: 11 March 2026

low- and high-NO_x conditions, Atmospheric Chemistry and Physics, 17, 159–174, https://doi.org/10.5194/acp-17-159-2017, 2017.

Dasari, S., Andersson, A., Bikkina, S., Holmstrand, H., Budhavant, K., Satheesh, S., Asmi, E., Kesti, J., Backman, J., Salam, A., Bisht, D. S., Tiwari, S., Hameed, Z., and Gustafsson, Ö.: Photochemical degradation affects the light absorption of water-soluble brown carbon in the South Asian outflow, Science Advances, 5, eaau8066, https://doi.org/10.1126/sciadv.aau8066, 2019.

Dasari, S., Andersson, A., Kim, S.-W., Holmstrand, H., Budhavant, K., and Gustafsson, Ö.: Observationally Constrained Wintertime Emission Fluxes and Atmospheric Lifetime of Black Carbon in South Asia, Environ. Sci. Technol. Lett., 12, 710–717, https://doi.org/10.1021/acs.estlett.5c00079, 2025.

DeCarlo, P. F., Kimmel, J. R., Trimborn, A., Northway, M. J., Jayne, J. T., Aiken, A. C., Gonin, M., Fuhrer, K., Horvath, T., Docherty, K. S., Worsnop, D. R., and Jimenez, J. L.: Field-Deployable, High-Resolution, Time-of-Flight Aerosol Mass Spectrometer, Anal. Chem., 78, 8281–8289, https://doi.org/10.1021/ac061249n, 2006.

Draxler, R. R. and Hess, G. D.: An overview of the HYSPLIT_4 modelling system for trajectories, dispersion and deposition, Australian Meteorological Magazine, 47, 295–308, 1998.

Ervens, B., Turpin, B. J., and Weber, R. J.: Secondary organic aerosol formation in cloud droplets and aqueous particles (aqSOA): a review of laboratory, field and model studies, Atmospheric Chemistry and Physics, 11, 11069–11102, https://doi.org/10.5194/acp-11-11069-2011, 2011.

Farmer, D. K., Matsunaga, A., Docherty, K. S., Surratt, J. D., Seinfeld, J. H., Ziemann, P. J., and Jimenez, J. L.: Response of an aerosol mass spectrometer to organonitrates and organosulfates and implications for atmospheric chemistry, Proceedings of the National Academy of Sciences, 107, 6670–6675, https://doi.org/10.1073/pnas.0912340107, 2010.

Feingold, G. and Kreidenweis, S.: Does cloud processing of aerosol enhance droplet concentrations?, Journal of Geophysical Research: Atmospheres, 105, 24351–24361, https://doi.org/10.1029/2000JD900369, 2000.

Gallimore, P. J., Achakulwisut, P., Pope, F. D., Davies, J. F., Spring, D. R., and Kalberer, M.: Importance of relative humidity in the oxidative ageing of organic aerosols: case study of the ozonolysis of maleic acid aerosol, Atmospheric Chemistry and Physics, 11, 12181–12195, https://doi.org/10.5194/acp-11-12181-2011, 2011.

Ganguly, D., Ray, R., Majumdar, N., Chowdhury, C., and Jana, T. K.: Biogenic hydrogen sulphide emissions and non-sea sulfate aerosols over the Indian Sundarban mangrove forest, J Atmos Chem, 75, 319–333, https://doi.org/10.1007/s10874-018-9382-3, 2018.

Giglio, L., Schroeder, W., and Justice, C. O.: The collection 6 MODIS active fire detection algorithm and fire products, Remote Sensing of Environment, 178, 31–41, https://doi.org/10.1016/j.rse.2016.02.054, 2016.

von Glasow, R. and Crutzen, P. J.: Model study of multiphase DMS oxidation with a focus on halogens, Atmospheric Chemistry and Physics, 4, 589–608, https://doi.org/10.5194/acp-4-589-2004, 2004.

https://doi.org/10.5194/egusphere-2026-914
Preprint. Discussion started: 11 March 2026

Granat, L., Engström, J. E., Praveen, S., and Rodhe, H.: Light absorbing material (soot) in rainwater and in aerosol particles in the Maldives, Journal of Geophysical Research: Atmospheres, 115, https://doi.org/10.1029/2009JD013768, 2010.

Hansen, A. M. K., Kristensen, K., Nguyen, Q. T., Zare, A., Cozzi, F., Nøjgaard, J. K., Skov, H., Brandt, J., Christensen, J. H., Ström, J., Tunved, P., Krejci, R., and Glasius, M.: Organosulfates and organic acids in Arctic aerosols: speciation, annual variation and concentration levels, Atmospheric Chemistry and Physics, 14, 7807–7823, https://doi.org/10.5194/acp-14-7807-2014, 2014.

Haslett, S. L., Bell, D. M., Kumar, V., Slowik, J. G., Wang, D. S., Mishra, S., Rastogi, N., Singh, A., Ganguly, D., Thornton, J., Zheng, F., Li, Y., Nie, W., Liu, Y., Ma, W., Yan, C., Kulmala, M., Daellenbach, K. R., Hadden, D., Baltensperger, U., Prevot, A. S. H., Tripathi, S. N., and Mohr, C.: Nighttime NO emissions strongly suppress chlorine and nitrate radical formation during the winter in Delhi, Atmospheric Chemistry and Physics, 23, 9023–9036, https://doi.org/10.5194/acp-23-9023-2023, 2023.

Hegde, P., Kawamura, K., Girach, I. A., and Nair, P. R.: Characterisation of water-soluble organic aerosols at a site on the southwest coast of India, J Atmos Chem, 73, 181–205, https://doi.org/10.1007/s10874-015-9322-4, 2016.

Hodshire, A. L., Campuzano-Jost, P., Kodros, J. K., Croft, B., Nault, B. A., Schroder, J. C., Jimenez, J. L., and Pierce, J. R.: The potential role of methanesulfonic acid (MSA) in aerosol formation and growth and the associated radiative forcings, Atmospheric Chemistry and Physics, 19, 3137–3160, https://doi.org/10.5194/acp-19-3137-2019, 2019.

Hoppel, W. A., Frick, G. M., Fitzgerald, J. W., and Larson, R. E.: Marine boundary layer measurements of new particle formation and the effects nonprecipitating clouds have on aerosol size distribution, Journal of Geophysical Research: Atmospheres, 99, 14443–14459, https://doi.org/10.1029/94JD00797, 1994.

Hsieh, L.-Y., Kuo, S.-C., Chen, C.-L., and Tsai, Y. I.: Origin of low-molecular-weight dicarboxylic acids and their concentration and size distribution variation in suburban aerosol, Atmospheric Environment, 41, 6648–6661, https://doi.org/10.1016/j.atmosenv.2007.04.014, 2007.

Japar, S. M., Wallington, T. J., Andino, J. M., and Ball, J. C.: Atmospheric chemistry of gaseous diethyl sulfate, Environ. Sci. Technol., 24, 894–897, https://doi.org/10.1021/es00076a017, 1990.

Kawamura, Kimitaka. and Kaplan, I. R.: Motor exhaust emissions as a primary source for dicarboxylic acids in Los Angeles ambient air, Environ. Sci. Technol., 21, 105–110, https://doi.org/10.1021/es00155a014, 1987.

Kleindienst, T. E., Jaoui, M., Lewandowski, M., Offenberg, J. H., Lewis, C. W., Bhave, P. V., and Edney, E. O.: Estimates of the contributions of biogenic and anthropogenic hydrocarbons to secondary organic aerosol at a southeastern US location, Atmospheric Environment, 41, 8288–8300, https://doi.org/10.1016/j.atmosenv.2007.06.045, 2007.

Krishnan, R. and Ramanathan, V.: Evidence of surface cooling from absorbing aerosols, Geophysical Research Letters, 29, 54-1-54–4, https://doi.org/10.1029/2002GL014687, 2002.

https://doi.org/10.5194/egusphere-2026-914
Preprint. Discussion started: 11 March 2026

Le Breton, M., Wang, Y., Hallquist, Å. M., Pathak, R. K., Zheng, J., Yang, Y., Shang, D., Glasius, M., Bannan, T. J., Liu, Q., Chan, C. K., Percival, C. J., Zhu, W., Lou, S., Topping, D., Wang, Y., Yu, J., Lu, K., Guo, S., Hu, M., and Hallquist, M.: Online gas- and particle-phase measurements of organosulfates, organosulfonates and nitrooxy organosulfates in Beijing utilizing a FIGAERO ToF-CIMS, Atmospheric Chemistry and Physics, 18, 10355–10371, https://doi.org/10.5194/acp-18-10355-2018, 2018.

Le Breton, M., Psichoudaki, M., Hallquist, M., Watne, Å. K., Lutz, A., and Hallquist, Å. M.: Application of a FIGAERO ToF CIMS for on-line characterization of real-world fresh and aged particle emissions from buses, Aerosol Science and Technology, 53, 244–259, https://doi.org/10.1080/02786826.2019.1566592, 2019.

Leck, C., Larsson, U., Bågander, L. E., Johansson, S., and Hajdu, S.: Dimethyl sulfide in the Baltic Sea: Annual variability in relation to biological activity, Journal of Geophysical Research: Oceans, 95, 3353–3363, https://doi.org/10.1029/JC095iC03p03353, 1990.

Li, X.-B., Yuan, B., Wang, S., Wang, C., Lan, J., Liu, Z., Song, Y., He, X., Huangfu, Y., Pei, C., Cheng, P., Yang, S., Qi, J., Wu, C., Huang, S., You, Y., Chang, M., Zheng, H., Yang, W., Wang, X., and Shao, M.: Variations and sources of volatile organic compounds (VOCs) in urban region: insights from measurements on a tall tower, Atmospheric Chemistry and Physics, 22, 10567–10587, https://doi.org/10.5194/acp-22-10567-2022, 2022.

Li, Y., Fu, T.-M., Yu, J. Z., Feng, X., Zhang, L., Chen, J., Boreddy, S. K. R., Kawamura, K., Fu, P., Yang, X., Zhu, L., and Zeng, Z.: Impacts of Chemical Degradation on the Global Budget of Atmospheric Levoglucosan and Its Use As a Biomass Burning Tracer, Environ. Sci. Technol., 55, 5525–5536, https://doi.org/10.1021/acs.est.0c07313, 2021a.

Li, Y., Zhao, J., Wang, Y., Seinfeld, J. H., and Zhang, R.: Multigeneration Production of Secondary Organic Aerosol from Toluene Photooxidation, Environ. Sci. Technol., 55, 8592–8603, https://doi.org/10.1021/acs.est.1c02026, 2021b.

Liu, S., Shilling, J. E., Song, C., Hiranuma, N., Zaveri, R. A., and Russell, L. M.: Hydrolysis of Organonitrate Functional Groups in Aerosol Particles, Aerosol Science and Technology, 46, 1359–1369, https://doi.org/10.1080/02786826.2012.716175, 2012.

Lopez-Hilfiker, F. D., Mohr, C., Ehn, M., Rubach, F., Kleist, E., Wildt, J., Mentel, T. F., Lutz, A., Hallquist, M., Worsnop, D., and Thornton, J. A.: A novel method for online analysis of gas and particle composition: description and evaluation of a Filter Inlet for Gases and AEROsols (FIGAERO), Atmospheric Measurement Techniques, 7, 983–1001, https://doi.org/10.5194/amt-7-983-2014, 2014.

Mackenzie-Rae, F. A., Wallis, H. J., Rickard, A. R., Pereira, K. L., Saunders, S. M., Wang, X., and Hamilton, J. F.: Ozonolysis of α-phellandrene – Part 2: Compositional analysis of secondary organic aerosol highlights the role of stabilised Criegee intermediates, Atmospheric Chemistry and Physics, 18, 4673–4693, https://doi.org/10.5194/acp-18-4673-2018, 2018.

Massoli, P., Stark, H., Canagaratna, M. R., Krechmer, J. E., Xu, L., Ng, N. L., Mauldin, R. L. I., Yan, C., Kimmel, J., Misztal, P. K., Jimenez, J. L., Jayne, J. T., and Worsnop, D. R.: Ambient Measurements of Highly Oxidized Gas-Phase Molecules during the Southern Oxidant and Aerosol Study (SOAS) 2013, ACS Earth Space Chem., 2, 653–672, https://doi.org/10.1021/acsearthspacechem.8b00028, 2018.

https://doi.org/10.5194/egusphere-2026-914
Preprint. Discussion started: 11 March 2026

Mehra, A., Wang, Y., Krechmer, J. E., Lambe, A., Majluf, F., Morris, M. A., Priestley, M., Bannan, T. J., Bryant, D. J., Pereira, K. L., Hamilton, J. F., Rickard, A. R., Newland, M. J., Stark, H., Croteau, P., Jayne, J. T., Worsnop, D. R., Canagaratna, M. R., Wang, L., and Coe, H.: Evaluation of the chemical composition of gas- and particle-phase products of aromatic oxidation, Atmospheric Chemistry and Physics, 20, 9783–9803, https://doi.org/10.5194/acp-20-9783-2020, 2020.

Meng, J., Wang, G., Li, J., Cheng, C., Ren, Y., Huang, Y., Cheng, Y., Cao, J., and Zhang, T.: Seasonal characteristics of oxalic acid and related SOA in the free troposphere of Mt. Hua, central China: Implications for sources and formation mechanisms, Science of The Total Environment, 493, 1088–1097, https://doi.org/10.1016/j.scitotenv.2014.04.086, 2014.

Middlebrook, A. M., Bahreini, R., Jimenez, J. L., and Canagaratna, M. R.: Evaluation of Composition-Dependent Collection Efficiencies for the Aerodyne Aerosol Mass Spectrometer using Field Data, Aerosol Science and Technology, 46, 258–271, https://doi.org/10.1080/02786826.2011.620041, 2012.

Mishra, S., Tripathi, S. N., Kanawade, V. P., Haslett, S. L., Dada, L., Ciarelli, G., Kumar, V., Singh, A., Bhattu, D., Rastogi, N., Daellenbach, K. R., Ganguly, D., Gargava, P., Slowik, J. G., Kulmala, M., Mohr, C., El-Haddad, I., and Prevot, A. S. H.: Rapid night-time nanoparticle growth in Delhi driven by biomass-burning emissions, Nat. Geosci., 16, 224–230, https://doi.org/10.1038/s41561-023-01138-x, 2023.

Nair, H. R. C. R., Budhavant, K., Manoj, M. R., Andersson, A., Satheesh, S. K., Ramanathan, V., and Gustafsson, Ö.: Aerosol demasking enhances climate warming over South Asia, npj Clim Atmos Sci, 6, 39, https://doi.org/10.1038/s41612-023-00367-6, 2023.

Nair, H. R. C. R., Budhavant, K., Manoj, M. R., Kirillova, E. N., Satheesh, S. K., and Gustafsson, Ö.: Roles of water-soluble aerosol coatings for the enhanced radiative absorption of black carbon over south asia and the northern indian ocean, Science of The Total Environment, 926, 171721, https://doi.org/10.1016/j.scitotenv.2024.171721, 2024.

Nakao, S., Clark, C., Tang, P., Sato, K., and Cocker III, D.: Secondary organic aerosol formation from phenolic compounds in the absence of NO_x, Atmospheric Chemistry and Physics, 11, 10649–10660, https://doi.org/10.5194/acp-11-10649-2011, 2011.

Nault, B. A., Croteau, P., Jayne, J., Williams, A., Williams, L., Worsnop, D., Katz, E. F., DeCarlo, P. F., and Canagaratna, M.: Laboratory evaluation of organic aerosol relative ionization efficiencies in the aerodyne aerosol mass spectrometer and aerosol chemical speciation monitor, Aerosol Science and Technology, 57, 981–997, https://doi.org/10.1080/02786826.2023.2223249, 2023.

Ng, N. L., Canagaratna, M. R., Jimenez, J. L., Chhabra, P. S., Seinfeld, J. H., and Worsnop, D. R.: Changes in organic aerosol composition with aging inferred from aerosol mass spectra, Atmospheric Chemistry and Physics, 11, 6465–6474, https://doi.org/10.5194/acp-11-6465-2011, 2011.

Nguyen, T. B., Bateman, A. P., Bones, D. L., Nizkorodov, S. A., Laskin, J., and Laskin, A.: High-resolution mass spectrometry analysis of secondary organic aerosol generated by ozonolysis of isoprene, Atmospheric Environment, 44, 1032–1042, https://doi.org/10.1016/j.atmosenv.2009.12.019, 2010.

https://doi.org/10.5194/egusphere-2026-914
Preprint. Discussion started: 11 March 2026

Nguyen, T. B., Roach, P. J., Laskin, J., Laskin, A., and Nizkorodov, S. A.: Effect of humidity on the composition of isoprene photooxidation secondary organic aerosol, Atmospheric Chemistry and Physics, 11, 6931–6944, https://doi.org/10.5194/acp-11-6931-2011, 2011.

Novakov, T., Andreae, M. O., Gabriel, R., Kirchstetter, T. W., Mayol-Bracero, O. L., and Ramanathan, V.: Origin of carbonaceous aerosols over the tropical Indian Ocean: Biomass burning or fossil fuels?, Geophysical Research Letters, 27, 4061–4064, https://doi.org/10.1029/2000GL011759, 2000.

Oghama, O. E., Voliotis, A., J. Bannan, T., A. Syafira, S., Hu, D., Wu, H., Gallimore, P., McFiggans, G., Coe, H., and D. Allan, J.: Variations in oxygenated and nitrogen-containing primary organic compounds based on the fuel type and burning condition in stove emissions, Environmental Science: Atmospheres, https://doi.org/10.1039/D5EA00080G, 2025.

Oh, B., Karin, P., Srilomsak, M., Chonvasin, K., Po-ngen, W., Srimanosaowapak, S., and Hanamura, K.: Characterization of biodiesels and tire derived particulate matters in morphology and nanostructure, Materials Today: Proceedings, 66, 2756–2761, https://doi.org/10.1016/j.matpr.2022.06.510, 2022.

Onasch, T. B., Trimborn, A., Fortner, E. C., Jayne, J. T., Kok, G. L., Williams, L. R., Davidovits, P., and Worsnop, D. R.: Soot Particle Aerosol Mass Spectrometer: Development, Validation, and Initial Application, Aerosol Science and Technology, 46, 804–817, https://doi.org/10.1080/02786826.2012.663948, 2012.

Papazian, S., D'Agostino, L. A., Sadiktsis, I., Froment, J., Bonnefille, B., Sdougkou, K., Xie, H., Athanassiadis, I., Budhavant, K., Dasari, S., Andersson, A., Gustafsson, Ö., and Martin, J. W.: Nontarget mass spectrometry and in silico molecular characterization of air pollution from the Indian subcontinent, Commun Earth Environ, 3, 35, https://doi.org/10.1038/s43247-022-00365-1, 2022.

Praplan, A. P., Hegyi-Gaeggeler, K., Barmet, P., Pfaffenberger, L., Dommen, J., and Baltensperger, U.: Online measurements of water-soluble organic acids in the gas and aerosol phase from the photooxidation of 1,3,5-trimethylbenzene, Atmospheric Chemistry and Physics, 14, 8665–8677, https://doi.org/10.5194/acp-14-8665-2014, 2014.

Ramachandran, S. and Rupakheti, M.: Year-round aerosol characteristics and radiative effects in the South Asian pollution outflow over a background site in the Maldives, Atmospheric Environment, 240, 117813, https://doi.org/10.1016/j.atmosenv.2020.117813, 2020.

Ramana, M. V. and Ramanathan, V.: Abrupt transition from natural to anthropogenic aerosol radiative forcing: Observations at the ABC-Maldives Climate Observatory, Journal of Geophysical Research: Atmospheres, 111, https://doi.org/10.1029/2006JD007063, 2006.

Reyes-Villegas, E., Bannan, T., Le Breton, M., Mehra, A., Priestley, M., Percival, C., Coe, H., and Allan, J. D.: Online Chemical Characterization of Food-Cooking Organic Aerosols: Implications for Source Apportionment, Environ. Sci. Technol., 52, 5308–5318, https://doi.org/10.1021/acs.est.7b06278, 2018.

Riva, M., Healy, R. M., Flaud, P.-M., Perraudin, E., Wenger, J. C., and Villenave, E.: Gas- and Particle-Phase Products from the Chlorine-Initiated Oxidation of Polycyclic Aromatic Hydrocarbons, J. Phys. Chem. A, 119, 11170–11181, https://doi.org/10.1021/acs.jpca.5b04610, 2015.

https://doi.org/10.5194/egusphere-2026-914
Preprint. Discussion started: 11 March 2026

Röhrl, A. and Lammel, G.: Determination of malic acid and other C4 dicarboxylic acids in atmospheric aerosol samples, Chemosphere, 46, 1195–1199, https://doi.org/10.1016/S0045-6535(01)00243-0, 2002.

Romanias, M. N., Coggon, M. M., Al Ali, F., Burkholder, J. B., Dagaut, P., Decker, Z., Warneke, C., Stockwell, C. E., Roberts, J. M., Tomas, A., Houzel, N., Coeur, C., and Brown, S. S.: Emissions and Atmospheric Chemistry of Furanoids from Biomass Burning: Insights from Laboratory to Atmospheric Observations, ACS Earth Space Chem., 8, 857–899, https://doi.org/10.1021/acsearthspacechem.3c00226, 2024.

Sáez Álvarez, P.: From maritime salvage to IMO 2020 strategy: Two actions to protect the environment, Marine Pollution Bulletin, 170, 112590, https://doi.org/10.1016/j.marpolbul.2021.112590, 2021.

Satheesh, S. K., Ramanathan, V., Li-Jones, X., Lobert, J. M., Podgorny, I. A., Prospero, J. M., Holben, B. N., and Loeb, N. G.: A model for the natural and anthropogenic aerosols over the tropical Indian Ocean derived from Indian Ocean Experiment data, Journal of Geophysical Research: Atmospheres, 104, 27421–27440, https://doi.org/10.1029/1999JD900478, 1999.

Sato, K., Ikemori, F., Ramasamy, S., Fushimi, A., Kumagai, K., Iijima, A., and Morino, Y.: Four- and Five-Carbon Dicarboxylic Acids Present in Secondary Organic Aerosol Produced from Anthropogenic and Biogenic Volatile Organic Compounds, Atmosphere, 12, 1703, https://doi.org/10.3390/atmos12121703, 2021.

Schwantes, R. H., Schilling, K. A., McVay, R. C., Lignell, H., Coggon, M. M., Zhang, X., Wennberg, P. O., and Seinfeld, J. H.: Formation of highly oxygenated low-volatility products from cresol oxidation, Atmospheric Chemistry and Physics, 17, 3453–3474, https://doi.org/10.5194/acp-17-3453-2017, 2017.

Sheesley, R. J., Andersson, A., and Gustafsson, Ö.: Source characterization of organic aerosols using Monte Carlo source apportionment of PAHs at two South Asian receptor sites, Atmospheric Environment, 45, 3874–3881, https://doi.org/10.1016/j.atmosenv.2011.01.031, 2011.

Siegel, K., Gramlich, Y., Haslett, S. L., Freitas, G., Krejci, R., Zieger, P., and Mohr, C.: Arctic observations of hydroperoxymethyl thioformate (HPMTF) – seasonal behavior and relationship to other oxidation products of dimethyl sulfide at the Zeppelin Observatory, Svalbard, Atmospheric Chemistry and Physics, 23, 7569–7587, https://doi.org/10.5194/acp-23-7569-2023, 2023.

Sorooshian, A., Varutbangkul, V., Brechtel, F. J., Ervens, B., Feingold, G., Bahreini, R., Murphy, S. M., Holloway, J. S., Atlas, E. L., Buzorius, G., Jonsson, H., Flagan, R. C., and Seinfeld, J. H.: Oxalic acid in clear and cloudy atmospheres: Analysis of data from International Consortium for Atmospheric Research on Transport and Transformation 2004, Journal of Geophysical Research: Atmospheres, 111, https://doi.org/10.1029/2005JD006880, 2006.

Souza, S. R., Vasconcellos, P. C., and Carvalho, L. R. F.: Low molecular weight carboxylic acids in an urban atmosphere: Winter measurements in São Paulo City, Brazil, Atmospheric Environment, 33, 2563–2574, https://doi.org/10.1016/S1352-2310(98)00383-5, 1999.

Spencer, M. T., Holecek, J. C., Corrigan, C. E., Ramanathan, V., and Prather, K. A.: Size-resolved chemical composition of aerosol particles during a monsoonal transition period over the Indian Ocean, Journal of Geophysical Research: Atmospheres, 113, https://doi.org/10.1029/2007JD008657, 2008.

https://doi.org/10.5194/egusphere-2026-914
Preprint. Discussion started: 11 March 2026

Srinivas, B. and Sarin, M. M.: Light absorbing organic aerosols (brown carbon) over the tropical Indian Ocean: impact of biomass burning emissions, Environ. Res. Lett., 8, 044042, https://doi.org/10.1088/1748-9326/8/4/044042, 2013.

Stein, A. F., Draxler, R. R., Rolph, G. D., Stunder, B. J. B., Cohen, M. D., and Ngan, F.: NOAA's HYSPLIT Atmospheric Transport and Dispersion Modeling System, Bulletin of the American Meteorological Society, 96, 2059–2077, https://doi.org/10.1175/BAMS-D-14-00110.1, 2015.

Stone, E. A., Yang, L., Yu, L. E., and Rupakheti, M.: Characterization of organosulfates in atmospheric aerosols at Four Asian locations, Atmospheric Environment, 47, 323–329, https://doi.org/10.1016/j.atmosenv.2011.10.058, 2012.

Szopa, S. V., Naik, B., Adhikary, P., Artaxo, T., Berntsen, T., Collins, W. D., Fuzzi, S., Gallardo, L., Kiendler-Scharr, A., Klimont, Z., Liao, H., Unger, N., and Zanis, P.: Short-Lived Climate Forcers, in: Climate Change 2021 – The Physical Science Basis: Working Group I Contribution to the Sixth Assessment Report of the Intergovernmental Panel on Climate Change, edited by: Masson-Delmotte, V., Zhai, P., Pirani, A., Connors, S. L., Péan, C., Berger, S., Caud, N., Chen, Y., Goldfarb, L., Gomis, M. I., Huang, M., Leitzell, K., Lonnoy, E., Matthews, J. B. R., Maycock, T. K., Waterfield, T., Yelekçi, R., Yu, R., and Zhou, B., Cambridge University Press, Cambridge, United Kingdom and New York, NY, USA, 817–922, https://doi.org/10.1017/9781009157896, 2023.

Veres, P., Roberts, J. M., Burling, I. R., Warneke, C., de Gouw, J., and Yokelson, R. J.: Measurements of gas-phase inorganic and organic acids from biomass fires by negative-ion proton-transfer chemical-ionization mass spectrometry, Journal of Geophysical Research: Atmospheres, 115, https://doi.org/10.1029/2010JD014033, 2010.

Wang, Y., Zhao, Y., Wang, Y., Yu, J.-Z., Shao, J., Liu, P., Zhu, W., Cheng, Z., Li, Z., Yan, N., and Xiao, H.: Organosulfates in atmospheric aerosols in Shanghai, China: seasonal and interannual variability, origin, and formation mechanisms, Atmospheric Chemistry and Physics, 21, 2959–2980, https://doi.org/10.5194/acp-21-2959-2021, 2021.

Xu, J., Tian, Y., Cheng, C., Wang, C., Lin, Q., Li, M., Wang, X., and Shi, G.: Characteristics and source apportionment of ambient single particles in Tianjin, China: The close association between oxalic acid and biomass burning, Atmospheric Research, 237, 104843, https://doi.org/10.1016/j.atmosres.2020.104843, 2020.

Yao, X., Fang, M., Chan, C. K., Ho, K. F., and Lee, S. C.: Characterization of dicarboxylic acids in PM2.5 in Hong Kong, Atmospheric Environment, 38, 963–970, https://doi.org/10.1016/j.atmosenv.2003.10.048, 2004.

Ye, C., Yuan, B., Lin, Y., Wang, Z., Hu, W., Li, T., Chen, W., Wu, C., Wang, C., Huang, S., Qi, J., Wang, B., Wang, C., Song, W., Wang, X., Zheng, E., Krechmer, J. E., Ye, P., Zhang, Z., Wang, X., Worsnop, D. R., and Shao, M.: Chemical characterization of oxygenated organic compounds in the gas phase and particle phase using iodide CIMS with FIGAERO in urban air, Atmospheric Chemistry and Physics, 21, 8455–8478, https://doi.org/10.5194/acp-21-8455-2021, 2021.

Yeatman, S. G., Spokes, L. J., and Jickells, T. D.: Comparisons of coarse-mode aerosol nitrate and ammonium at two polluted coastal sites, Atmospheric Environment, 35, 1321–1335, https://doi.org/10.1016/S1352-2310(00)00452-0, 2001.

https://doi.org/10.5194/egusphere-2026-914
Preprint. Discussion started: 11 March 2026

Yee, L. D., Kautzman, K. E., Loza, C. L., Schilling, K. A., Coggon, M. M., Chhabra, P. S., Chan, M. N., Chan, A. W. H., Hersey, S. P., Crounse, J. D., Wennberg, P. O., Flagan, R. C., and Seinfeld, J. H.: Secondary organic aerosol formation from biomass burning intermediates: phenol and methoxyphenols, Atmospheric Chemistry and Physics, 13, 8019–8043, https://doi.org/10.5194/acp-13-8019-2013, 2013.

Yu, J. Z., Huang, X.-F., Xu, J., and Hu, M.: When Aerosol Sulfate Goes Up, So Does Oxalate: Implication for the Formation Mechanisms of Oxalate, Environ. Sci. Technol., 39, 128–133, https://doi.org/10.1021/es049559f, 2005.

Zhang, Q., Jimenez, J. L., Worsnop, D. R., and Canagaratna, M.: A Case Study of Urban Particle Acidity and Its Influence on Secondary Organic Aerosol, Environ. Sci. Technol., 41, 3213–3219, https://doi.org/10.1021/es061812j, 2007.

Zhao, R., Mungall, E. L., Lee, A. K. Y., Aljawhary, D., and Abbatt, J. P. D.: Aqueous-phase photooxidation of levoglucosan – a mechanistic study using aerosol time-of-flight chemical ionization mass spectrometry (Aerosol ToF-CIMS), Atmospheric Chemistry and Physics, 14, 9695–9706, https://doi.org/10.5194/acp-14-9695-2014, 2014.

Zorn, S. R., Drewnick, F., Schott, M., Hoffmann, T., and Borrmann, S.: Characterization of the South Atlantic marine boundary layer aerosol using an aerodyne aerosol mass spectrometer, Atmospheric Chemistry and Physics, 8, 4711–4728, https://doi.org/10.5194/acp-8-4711-2008, 2008.